Supporting Information

A New Echelon of Precision Polypentenamers: Highly Isotactic Branching on Every Five Carbons

Stefan Brits, William J. Neary, Goutam Palui, & Justin G. Kennemur

Department of Chemistry and Biochemistry, Florida State University, Tallahassee, FL 32306, USA

Table of Contents:

Synthesis of Mosher acid and DACH-Phenyl Trost Ligand S3
Figure SI-1. ^{1}H NMR spectra of *rac*-1 S4
Figure SI-2. ^{13}C NMR spectra of *rac*-1 S5
Figure SI-3. ^{1}H-^{1}H COSY spectra of *rac*-1 S6
Figure SI-4. GC-EI/MS of *rac*-1 S7
Figure SI-5. ^{1}H NMR spectra of *rac*-3 S8
Figure SI-6. ^{13}C NMR spectra of *rac*-3 S9
Figure SI-7. ^{1}H-^{1}H COSY spectra of *rac*-3 S10
Figure SI-8. GC-EI/MS of *rac*-3 S11
Figure SI-9. ^{1}H NMR spectra of *rac*-2 S12
Figure SI-10. ^{13}C NMR spectra of *rac*-2 S13
Figure SI-11. ^{1}H-^{1}H COSY spectra of *rac*-2 S14
Figure SI-12. GC-EI/MS of *rac*-2 S15
Figure SI-13. ^{1}H NMR spectra of *rac*-4 S16
Figure SI-14. ^{13}C NMR spectra of *rac*-4 S17
Figure SI-15. ^{1}H-^{1}H COSY spectra of *rac*-4 S18
Figure SI-16. GC-EI/MS of *rac*-4 S19
Figure SI-17. ^{1}H NMR spectra of (S)-1 S20
Figure SI-18. ^{13}C NMR spectra of (S)-1 S21
Figure SI-19. GC-EI/MS of (*S*)-1 S22
Figure SI-20. ^{1}H NMR spectra of (S)-2-MTPACP ester S23
Figure SI-21. ^{1}H-^{1}H COSY spectra of (S)-2-MTPACP ester S24

Figure SI-22. ^{1}H NMR spectra of (S)-2-MTPACP ester for % enantiomeric excess S25
Figure SI-23. ^{19}F NMR of (S)-2-MTPACP ester for % enantiomeric excess S26
Figure SI-24. ^{1}H NMR of (*S*)-3 S27
Figure SI-25. ^{13}C NMR of (*S*)-3 S28
Figure SI-26. GC-EI/MS of (*S*)-3 S29
Figure SI-27. ^{1}H NMR spectra of (R, R)-DACH Phenyl Trost ligand S30
Figure SI-28. ^{13}C NMR spectra of (R, R)-DACH Phenyl Trost ligand S31
Figure SI-29. ^{31}P NMR spectra of (R, R)-DACH Phenyl Trost ligand S32
Figure SI-30. ^{1}H NMR spectra of Poly[(S)-3] S33
Figure SI-31. ^{13}C NMR spectra of Poly[(S)-3] S34
Figure SI-32. ^{1}H-^{1}H COSY spectra of Poly[(S)-3] S35
Figure SI-33. ^{1}H-NMR of Poly(*S*)-3 determination %HT and % trans. S36
Figure SI-34. SEC RI trace of Poly(*S*)-3. S37
Figure SI-35. ^{1}H NMR of spectra of Poly(rac-3) S38
Figure SI-36. ^{13}C NMR of spectra of Poly(rac-3) S39
Figure SI-37. ^{1}H-^{1}H COSY of spectra of Poly(rac-3) S40
Figure SI-38. ^{1}H-NMR of Poly(*rac*-3) determination %HT and % trans. S41
Figure SI-39. SEC RI trace of Poly(*rac*-3). S42
Figure SI-40. ^{1}H NMR spectra of Poly(rac-2) S43
Figure SI-41. ^{13}C NMR spectra of Poly(rac-2) S44
Figure SI-42. ^{1}H-^{1}H COSY spectra of Poly(rac-2) S45
Figure SI-43. ^{1}H-NMR of Poly(*rac*-2) determination %HT and % trans. S46
Figure SI-44. SEC RI trace of Poly(*rac*-2). S47
Figure SI-45. ^{1}H NMR spectra of Poly(rac-1) S48
Figure SI-46. ^{13}C NMR spectra of Poly(rac-1) S49
Figure SI-47. ^{1}H-^{1}H COSY spectra of Poly(rac-1) S50
Figure SI-48. ^{1}H-NMR of Poly(*rac*-2) determination %HT and % trans. S51
Table SI-49. Equilibrium conversion of Poly(*rac*-3) S52
Figure SI-50. Conversion vs. time of Poly(*rac*-3) S53
Figure SI-51. TGA curve of Poly(*rac*-1), poly(*rac*-2), and poly(rac-3) S54
Figure SI-52. DSC overlay of all polymer samples S55

Mosher acid synthesis for the determination of % enantiomeric excess:[1]

To a flame dried 4mL vial equipped with a stir bar, 7.1 mg (84.4 µmol, 1 eq.) of (S)-1 and 1.00 mL of DCM that was previously run through a plug of silica gel were added. To a separate dry vial, 0.0613 g (261.6 µmol, 3.1 eq.) of (R)-(+)-α-methoxy-α-trifluoromethylphenylacetic was added and dissolved in 0.32 mL of DCM. This solution was then added to (S)-1. To the solution, 0.0545g (261.4 µmol, 3.1 eq.) of DCC and 0.0323g (261.4 µmol, 3.1 eq.) of DMAP were added and capped. The mixture was allowed to stir for 3 hours. At this time, the mixture was run through a cotton plug and concentrated. The mixture was purified with a pipet column in 4:1 hexanes:EtOAc. The product was then concentrated and placed on the high-vacuum for 30 minutes. ^{1}H NMR (400 MHz, $CDCl_3$) δ (ppm): 7.51 (m, 2H), 7.40 (m, 3H), 6.15 (ddd, J = 5.7, 2.6, 1.6 Hz, 1H), 5.92 (m, 1H), 5.86 (m, 1H), 3.55 (s, 1H), 2.50 (dtdd, J = 15.8, 8.9, 4.2, 2.4 Hz, 1H), 2.37 (m, 2H), 1.95 (m, 1H)

(R, R)-DACH Phenyl Trost ligand:[2, 3]

The Trost ligand was synthesized following previous literature[1] with the following modifications. The brown solid was purified with 97.5:2.5 DCM:MeOH via column chromatography and recrystallized twice from MeCN to yield a white solid. ^{1}H NMR (600 MHz, $CDCl_3$) δ (ppm): 7.60 – 7.55 (m, 2H), 7.35 – 7.17 (m, 24H), 6.94 – 6.88 (m, 2H), 6.32 (d, J = 6.9 Hz, 2H), 3.82 – 3.73 (m, 2H), 1.90 – 1.82 (m, 2H), 1.69 – 1.61 (m, 2H), 1.28 – 1.15 (m, 2H), 0.98 (td, J = 15.1, 13.8, 6.2 Hz, 2H). ^{13}C NMR (150 MHz, $CDCl_3$) δ (ppm): 169.29, 140.88, 140.72, 137.84, 137.76, 137.70, 136.73, 136.58, 134.27, 133.95, 133.82, 130.16, 128.75, 128.60, 128.54, 128.51, 128.49, 128.45, 128.40, 53.89, 32.00, 24.66. ^{31}P NMR (243 MHz, $CDCl_3$) δ -9.78.

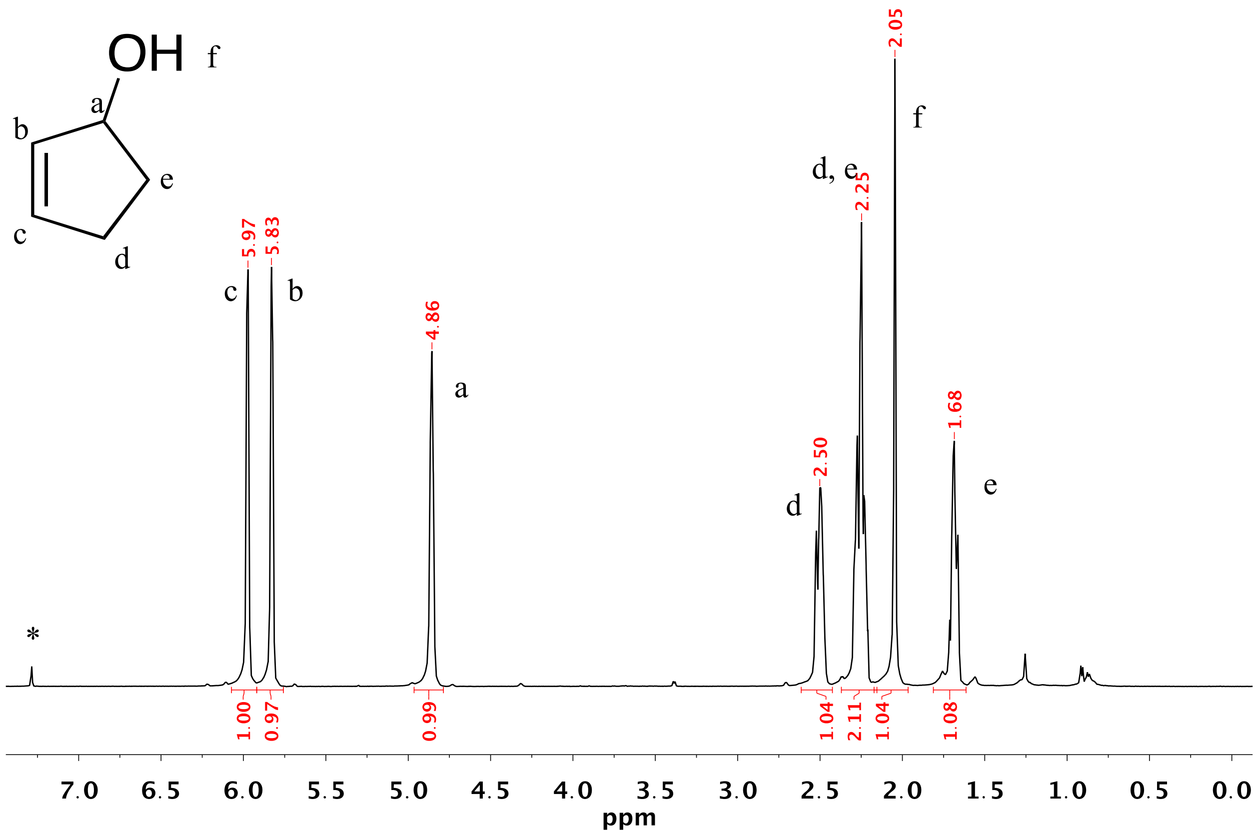

Figure S1. ^{1}H-NMR spectrum of *rac*-1, (in *$CDCl_3$ 400 MHz)

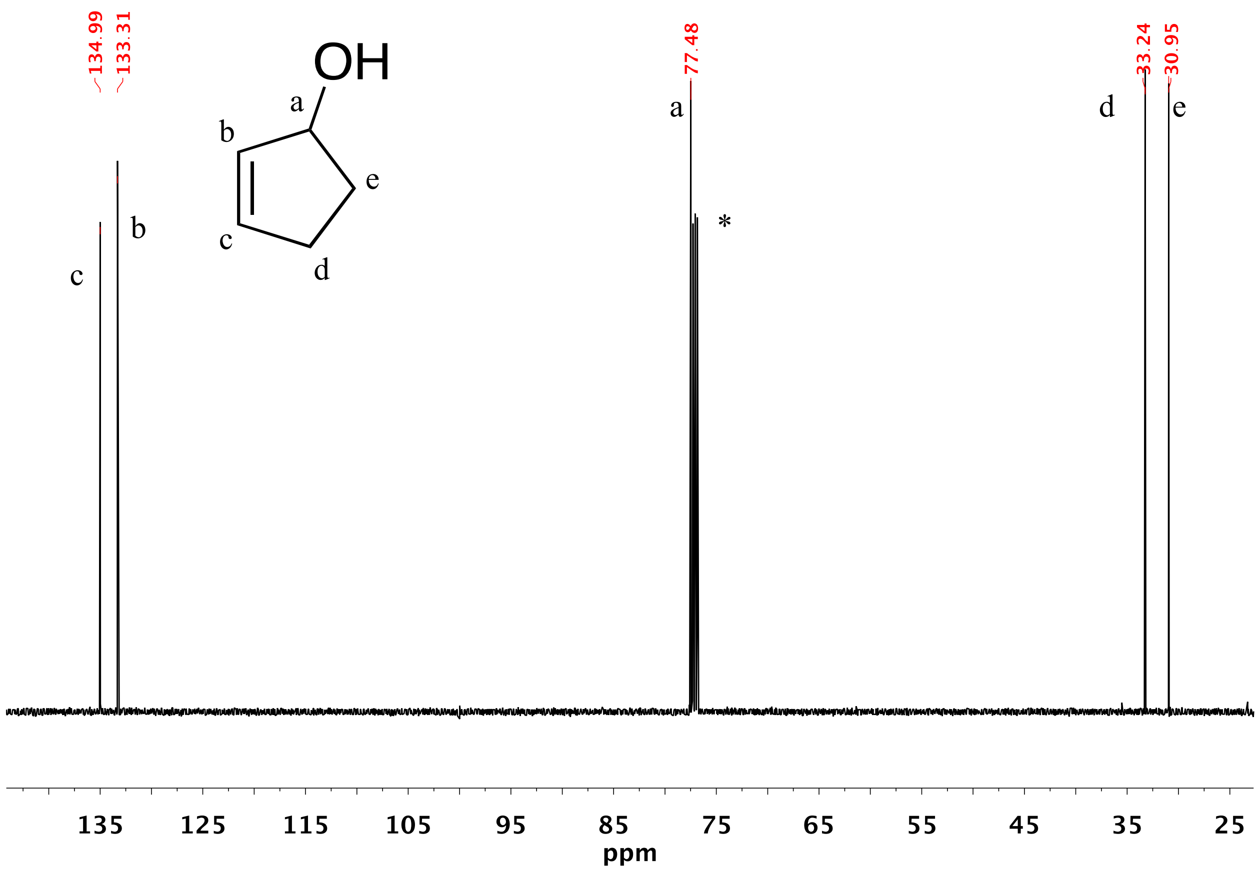

Figure S2. ^{13}C-NMR spectrum of *rac*-1, (in *$CDCl_3$ 150 MHz)

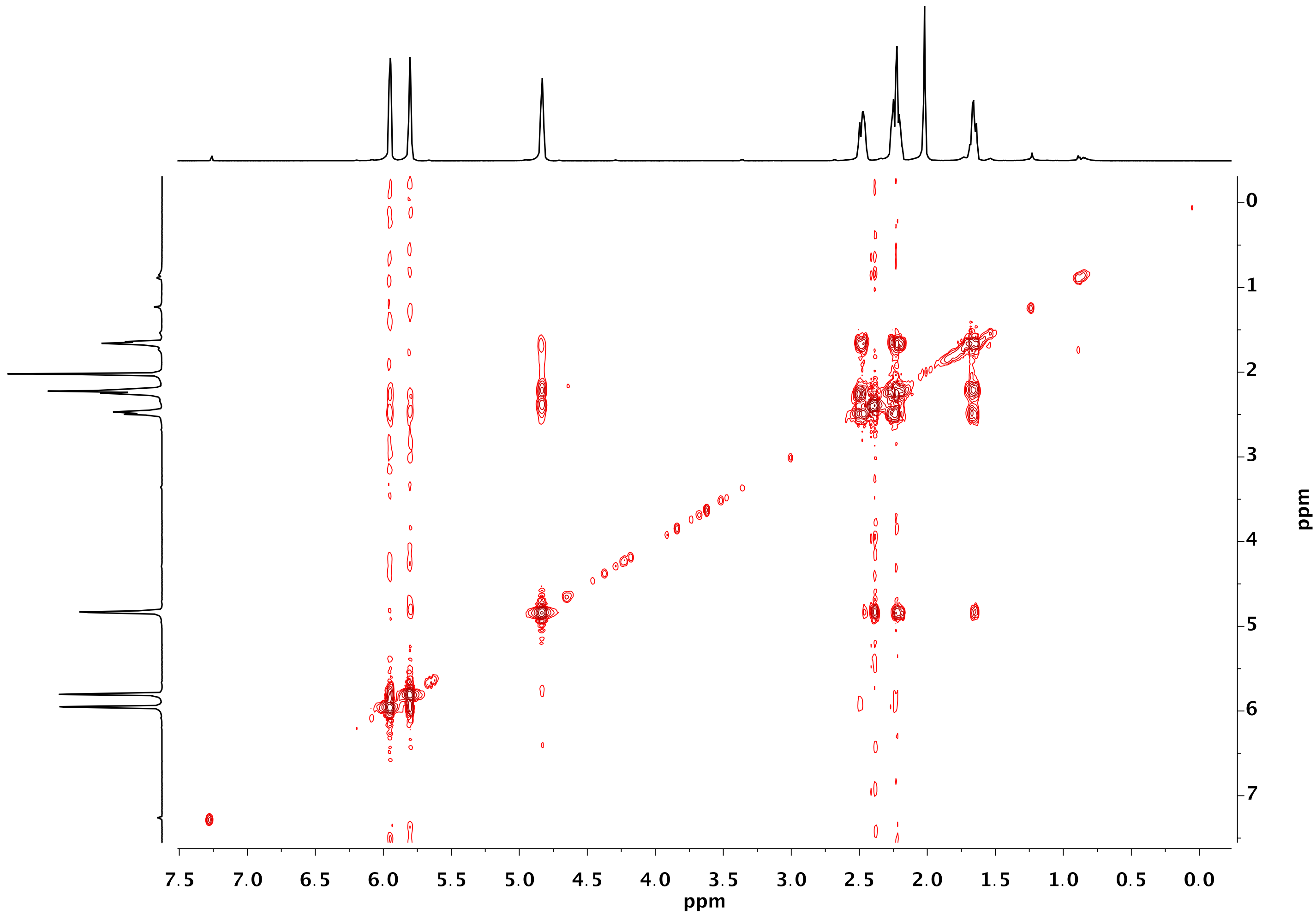

Figure S3. ^{1}H-^{1}H COSY spectrum of *rac*-1, (in $CDCl_3$ 600 MHz)

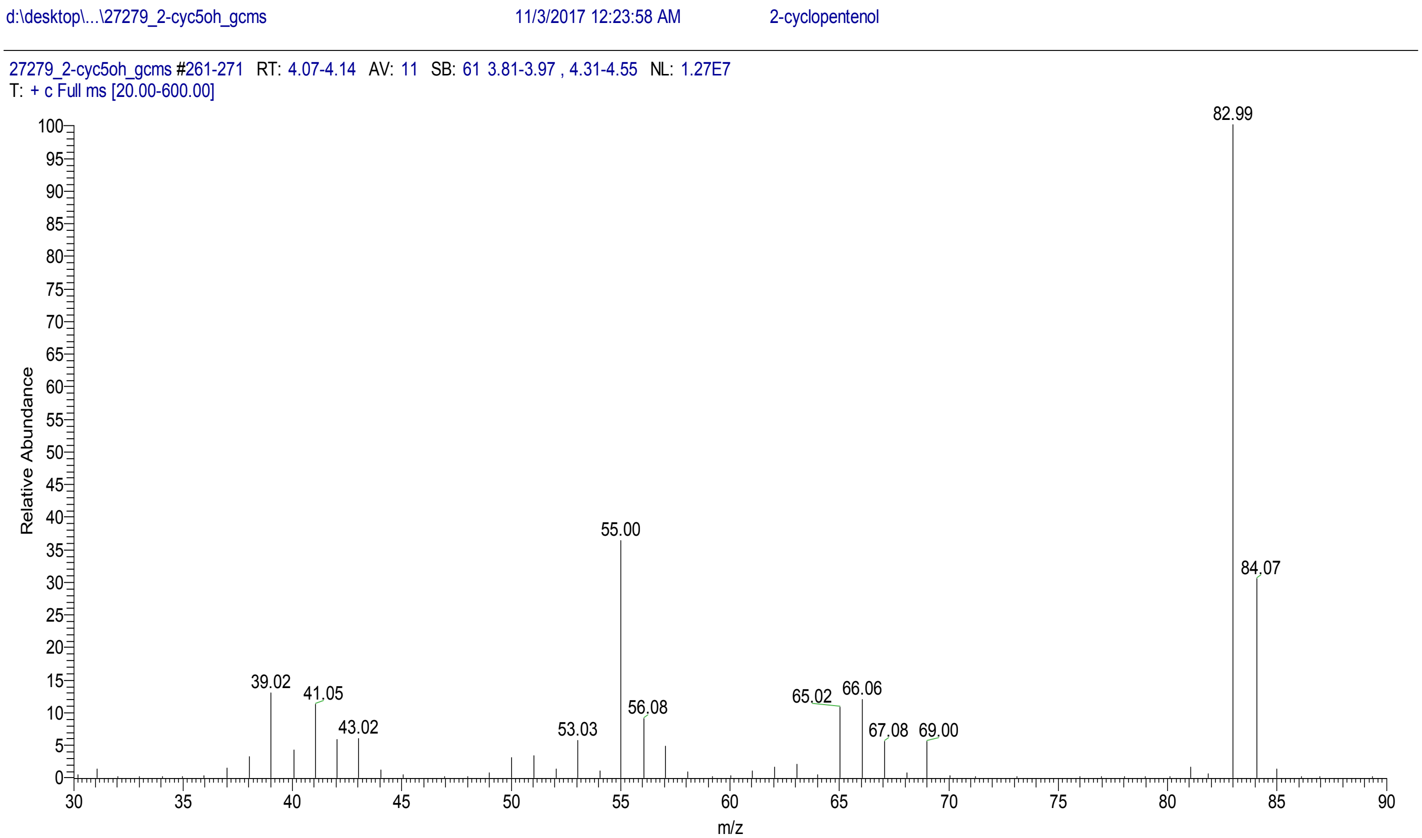

Figure S4. The mass spectrum at RT 4.08-4.12 min for *rac*-1. The molecular peak is observed at *m/z* 84.07.

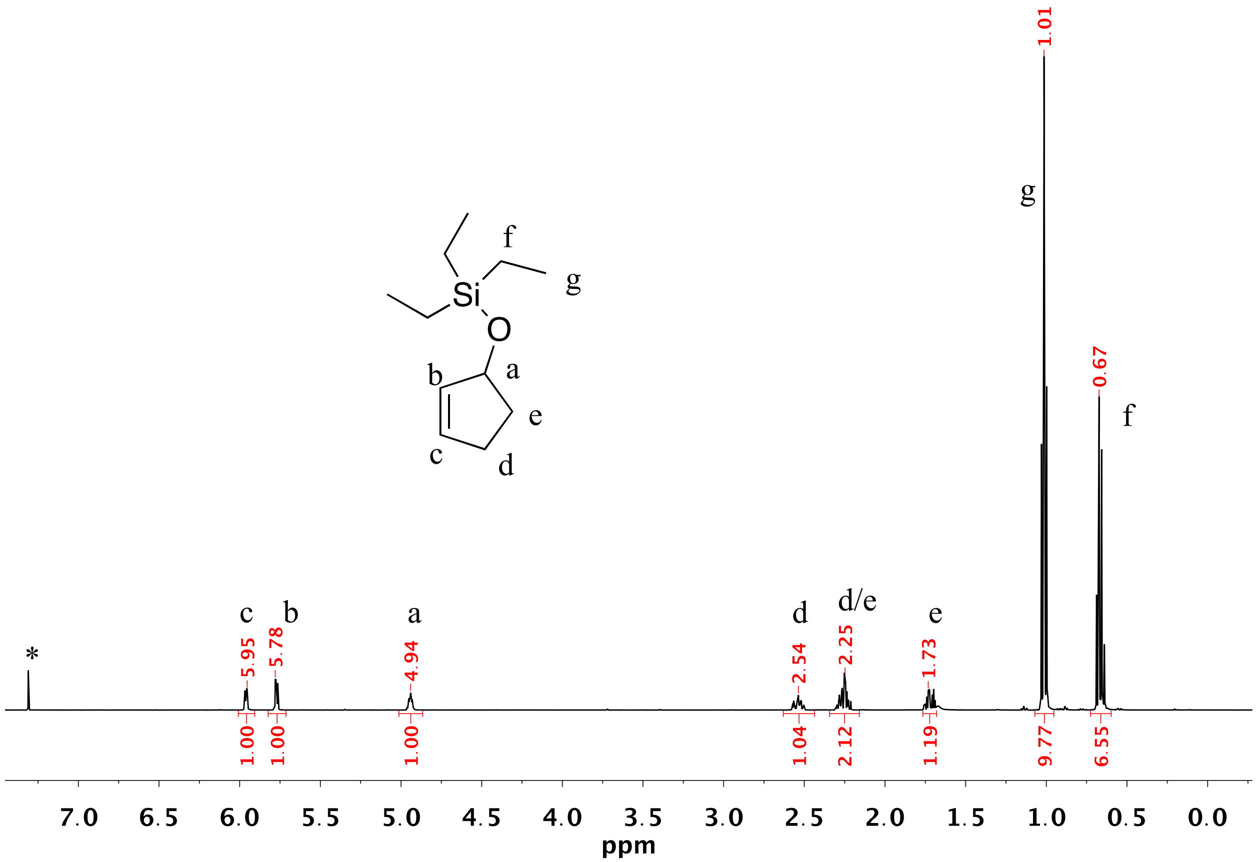

Figure S5. ¹H-NMR spectrum of *rac*-3, (in *$CDCl_3$ 500 MHz).

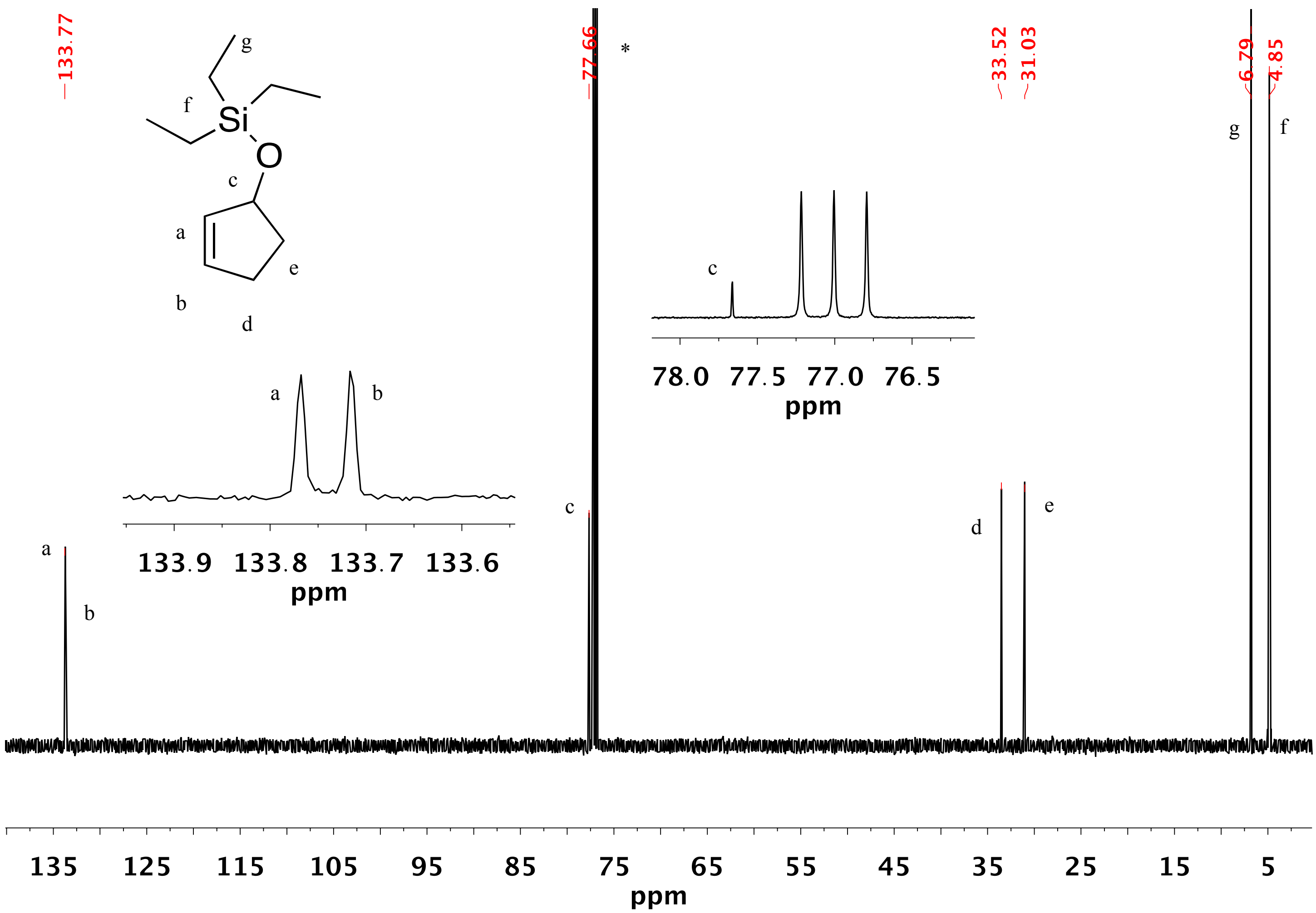

Figure S6. ^{13}C-NMR spectrum of *rac*-3, (in *$CDCl_3$ 150 MHz)

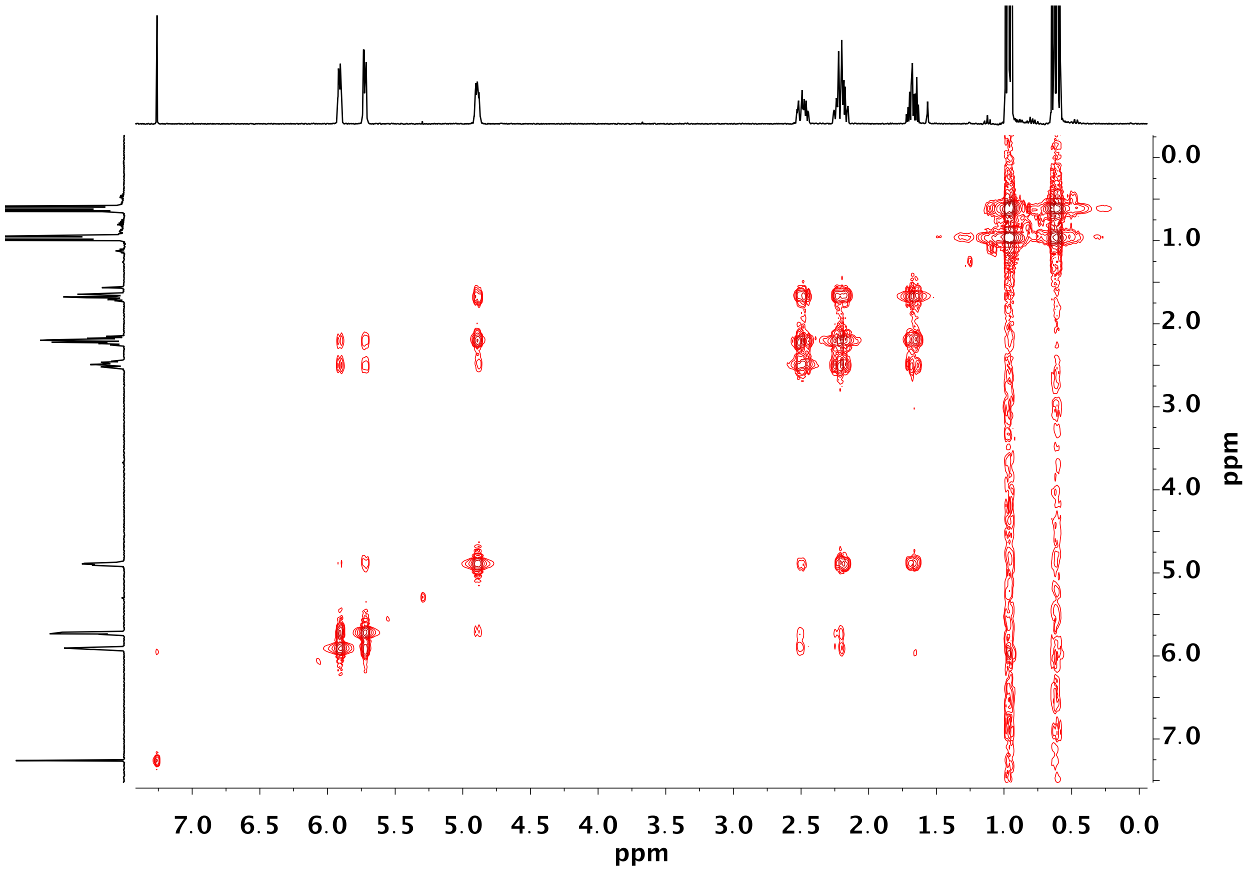

Figure S7. ^{1}H-^{1}H COSY spectrum of *rac*-3, (in $CDCl_3$ 500 MHz).

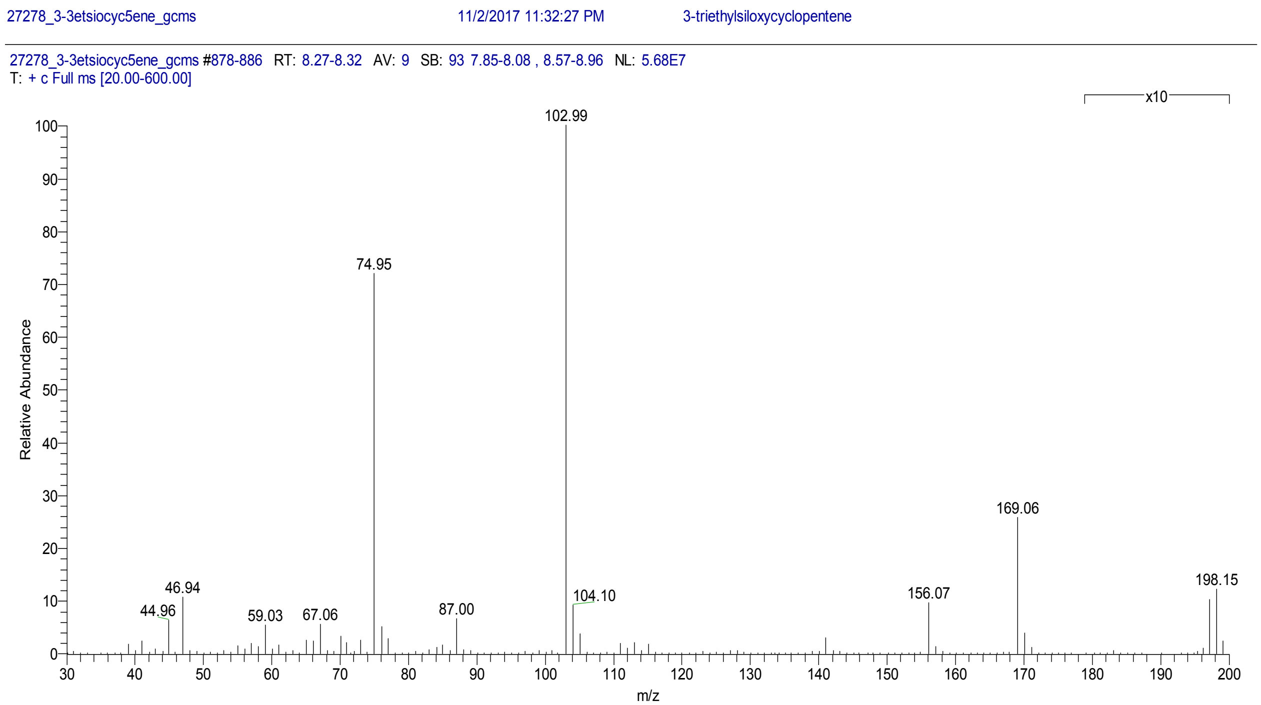

Figure S8: The mass spectrum at RT 8.27-8.32 min for the sample *rac*-3 The molecular peak is observed at *m/z* 198.15.

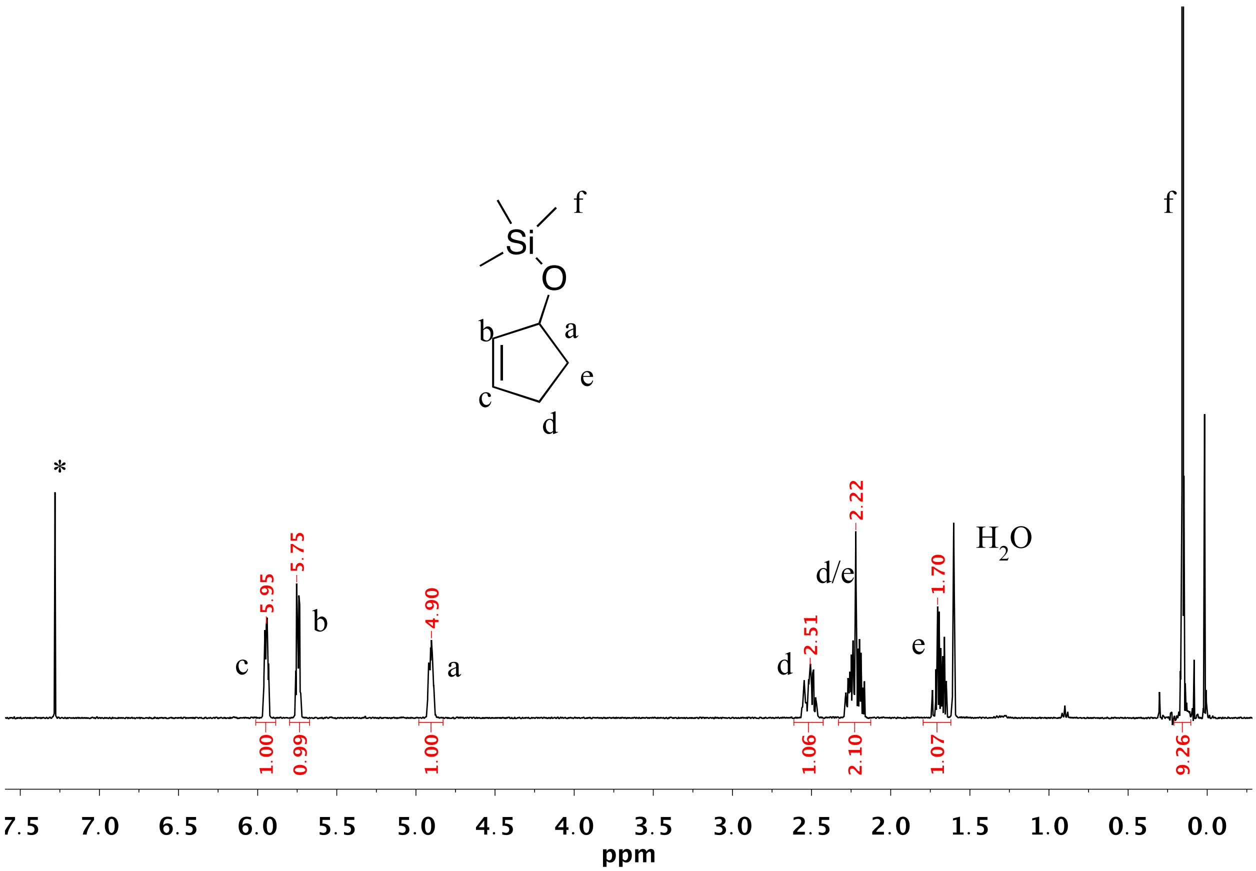

Figure S9. [1]H-NMR spectrum of *rac*-2, (in *$CDCl_3$ 400 MHz)

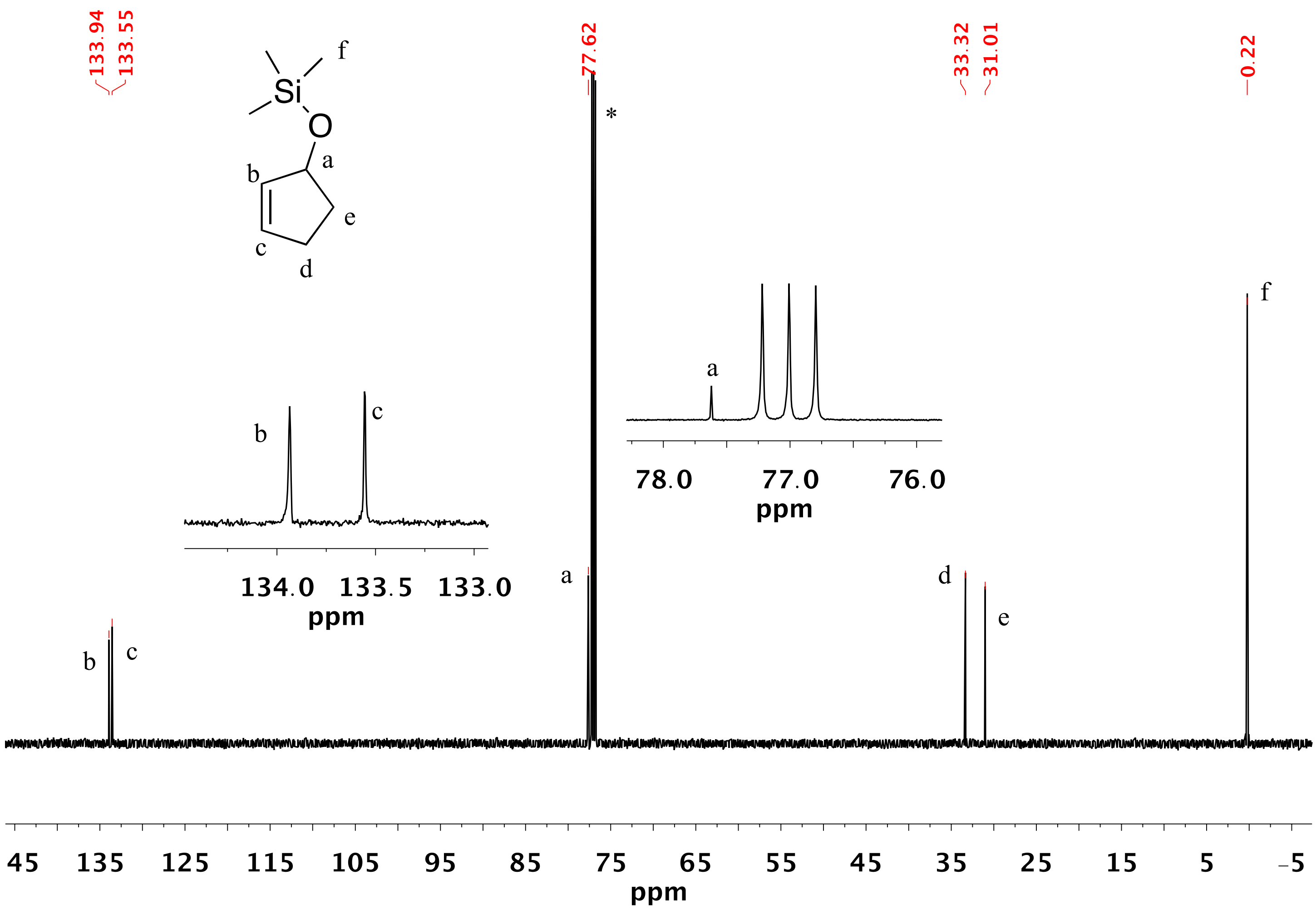

Figure S10. ^{13}C-NMR spectrum of *rac*-2, (in *$CDCl_3$ 150 MHz)

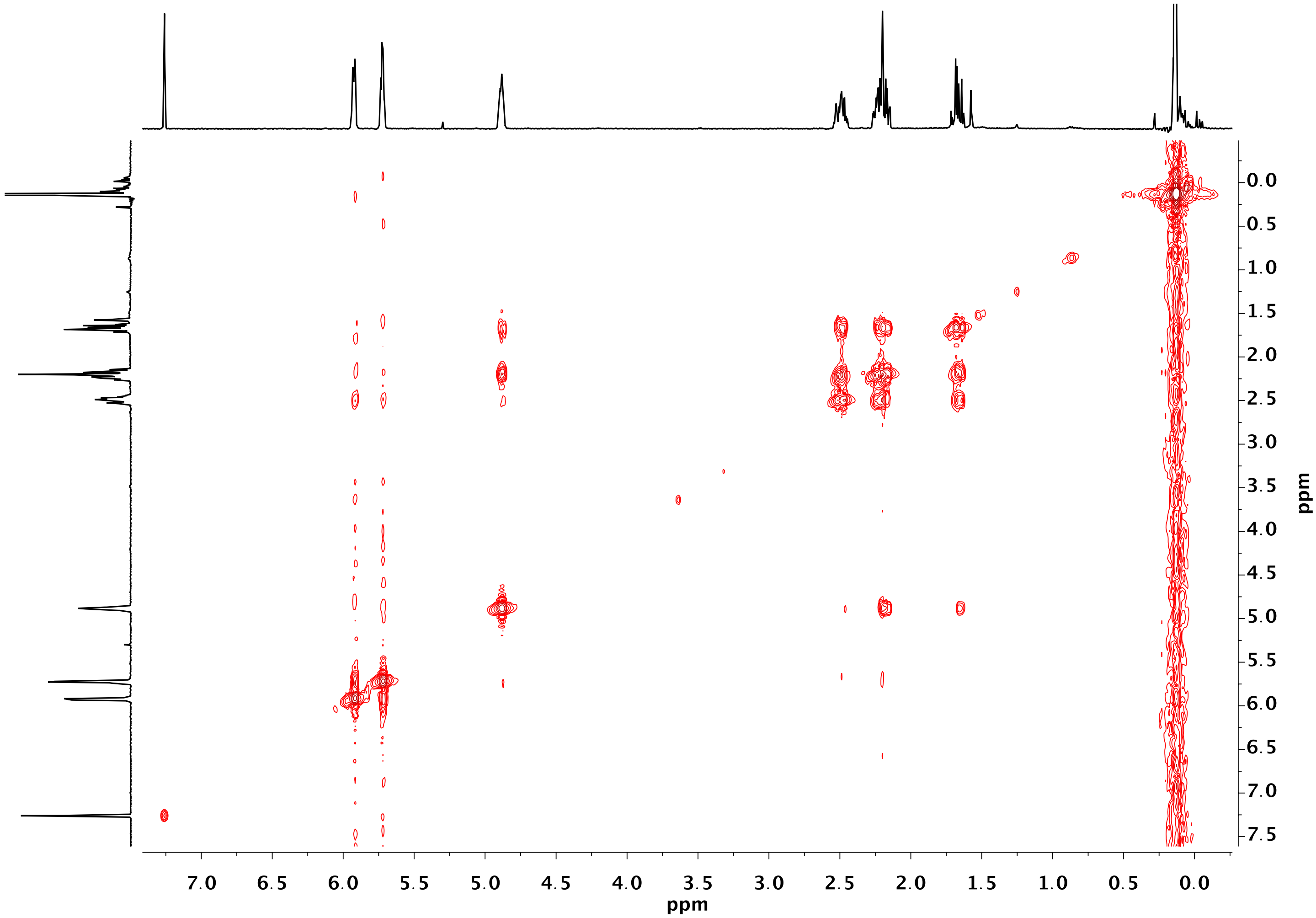

Figure S11. ^{1}H-^{1}H COSY spectrum of *rac*-2, (in $CDCl_3$ 600 MHz)

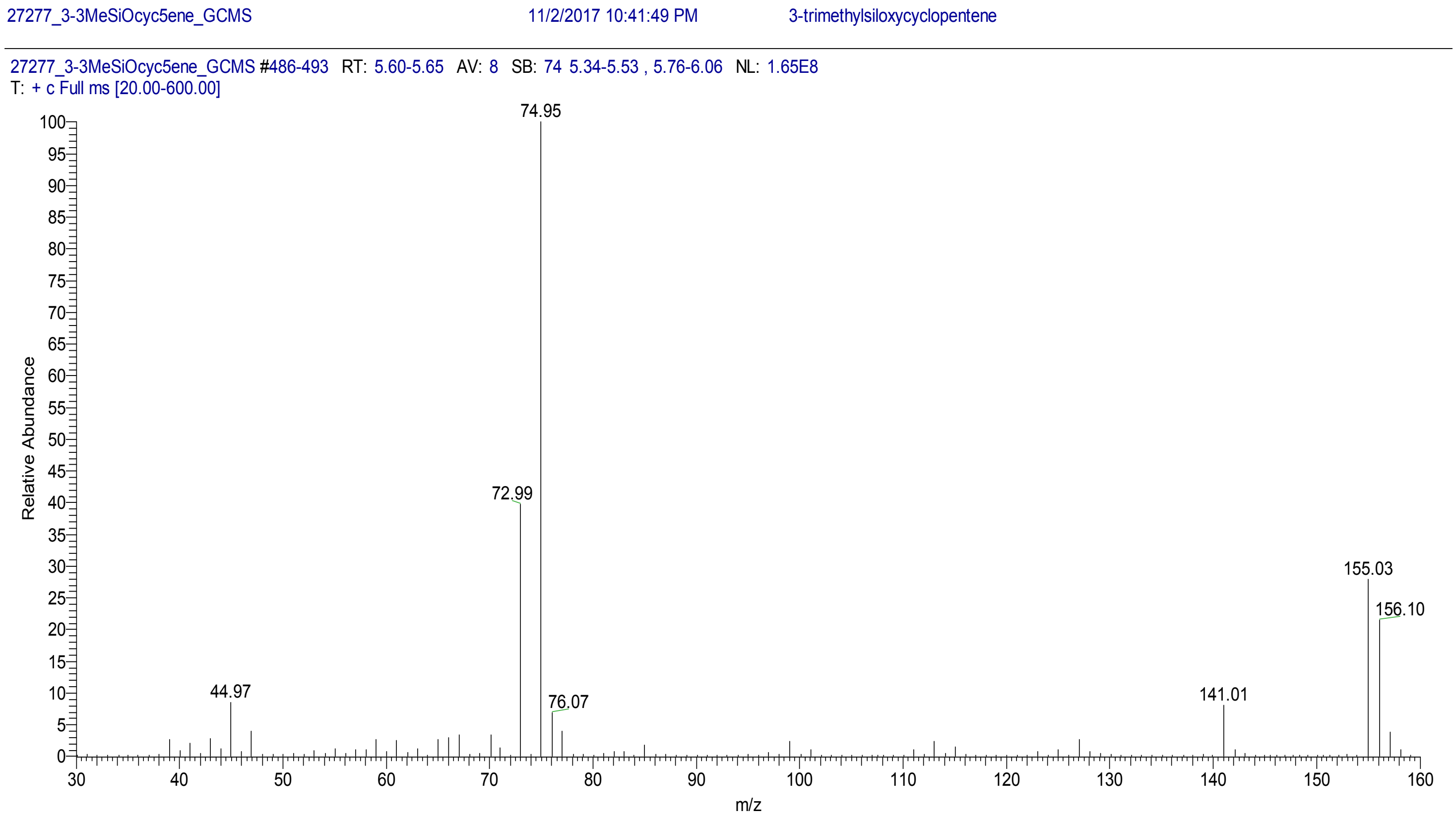

Figure S12. The mass spectrum at RT 5.60-5.65 min for the sample *rac*-2. The molecular peak is observed at *m/z* 156.10.

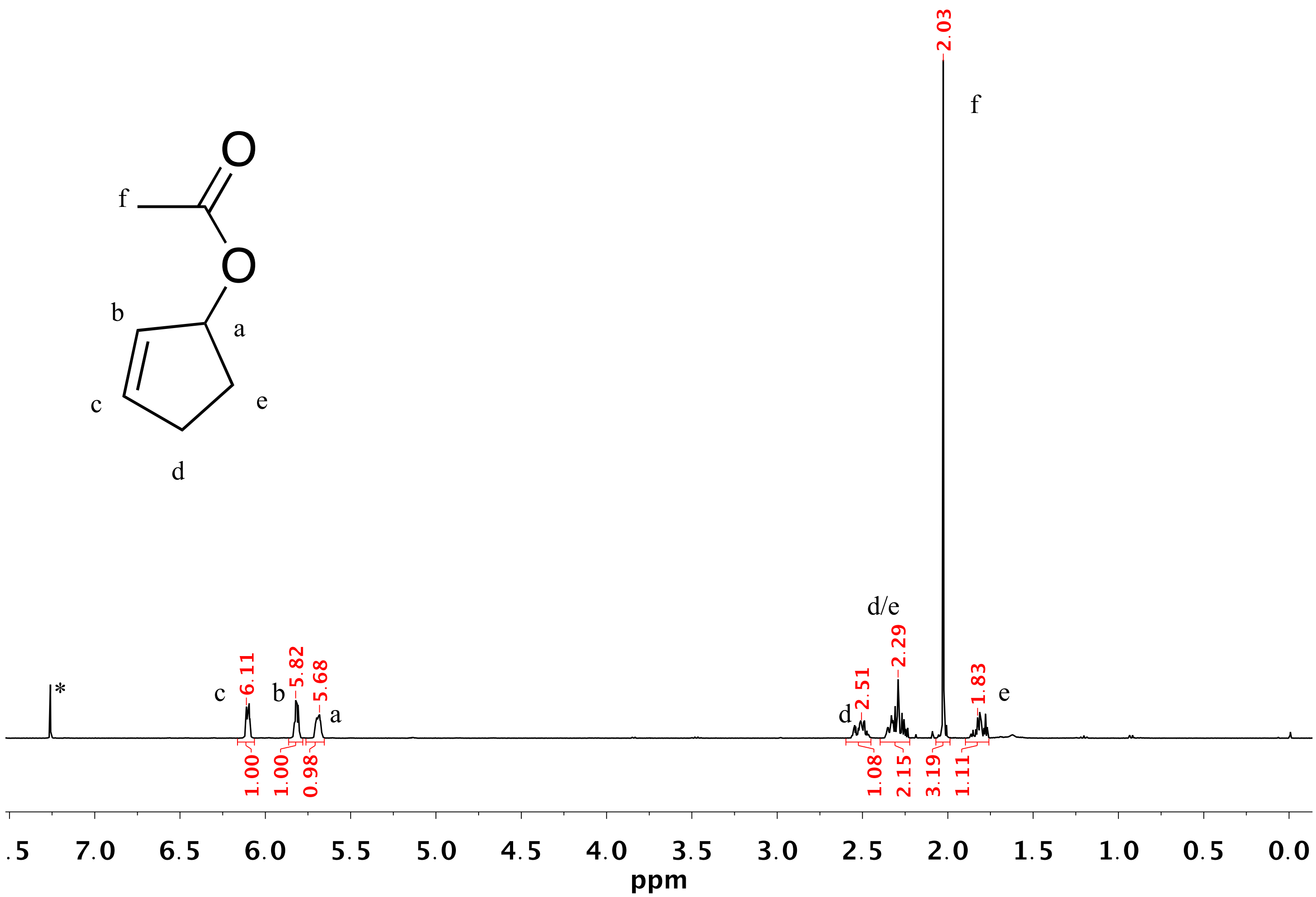

Figure S13. ^{1}H-NMR spectrum of *rac*-4, (in *$CDCl_3$ 400 MHz)

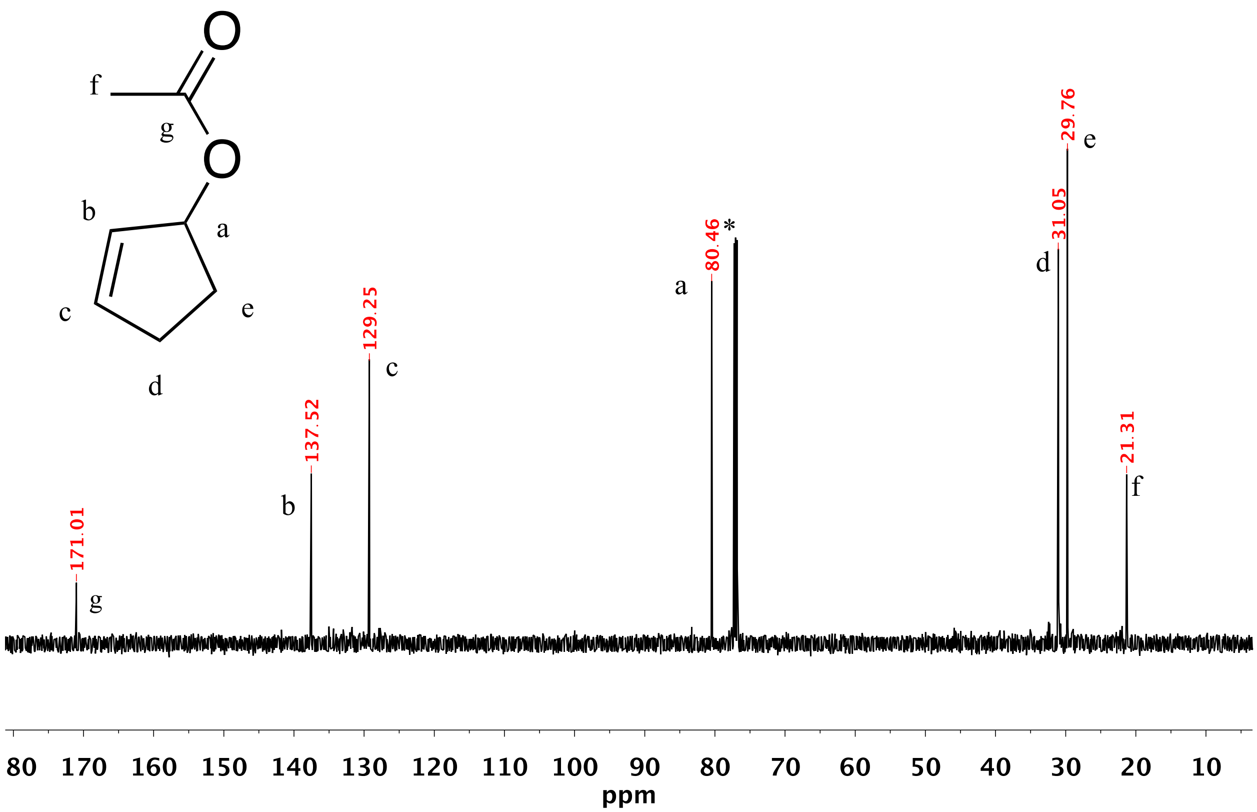

Figure S14. ^{13}C-NMR spectrum of *rac*-4, (in *$CDCl_3$, 150 MHz)

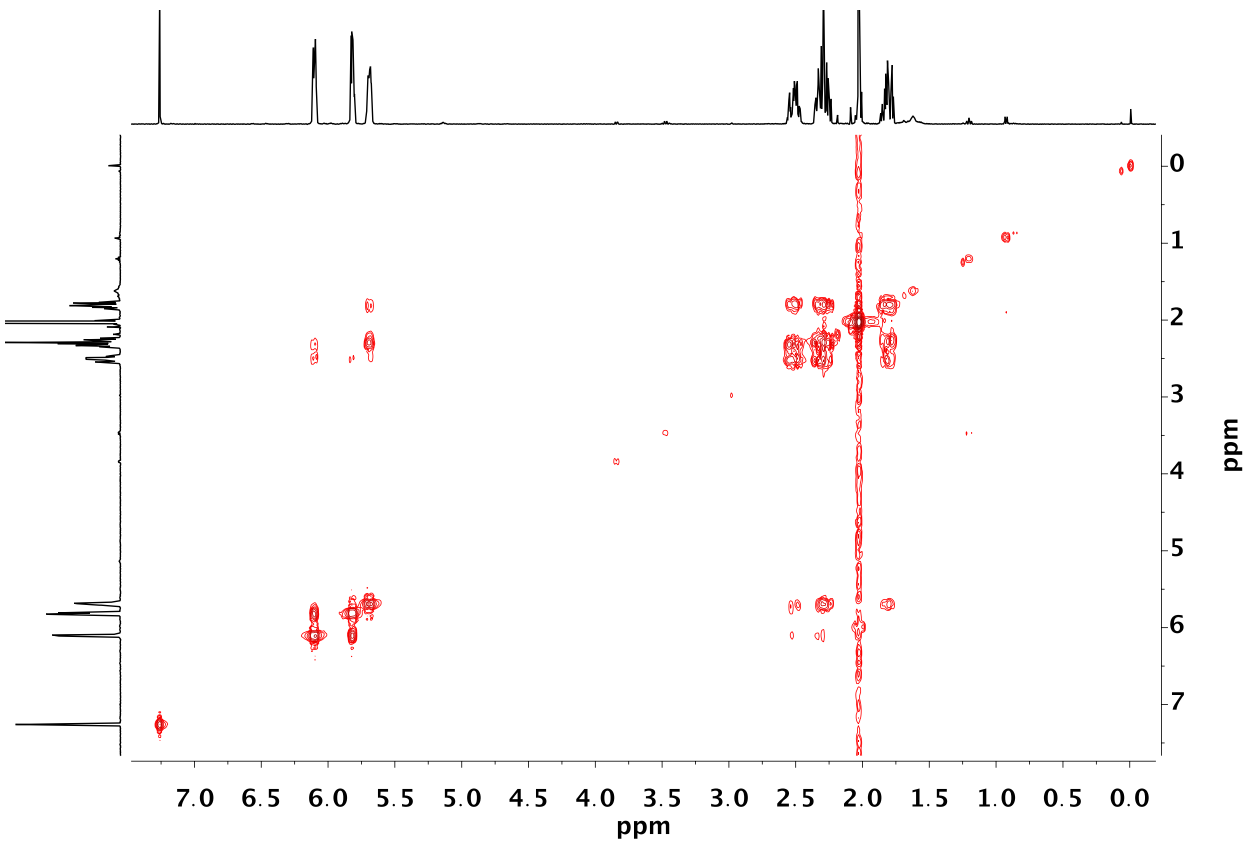

Figure S15. ^{1}H-^{1}H COSY spectrum of *rac*-4, (in $CDCl_3$ 600 MHz)

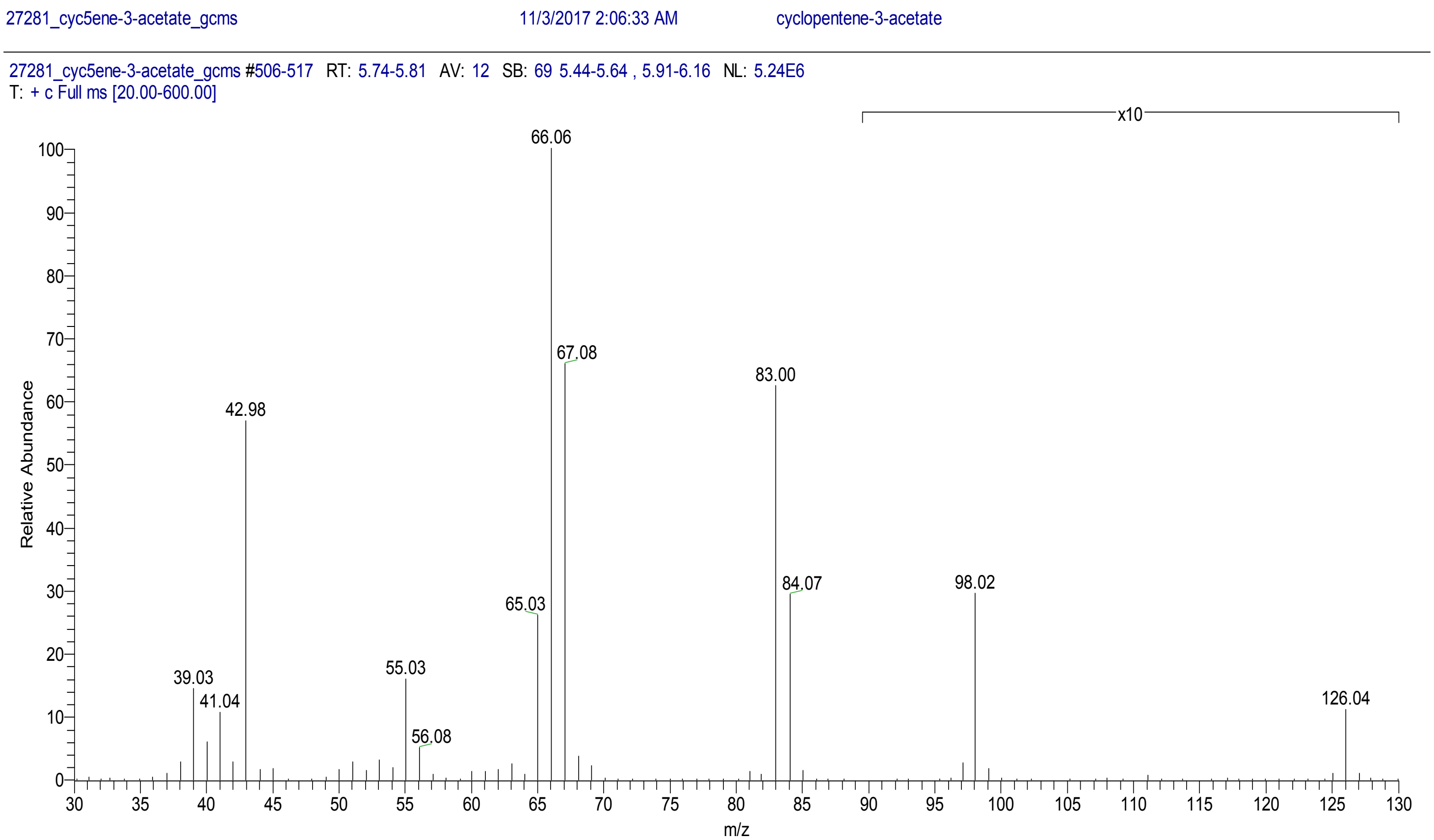

Figure S16: The mass spectrum at RT 5.74-5.81 min of *rac*-4. The molecular peak is observed at *m/z* 126.04.

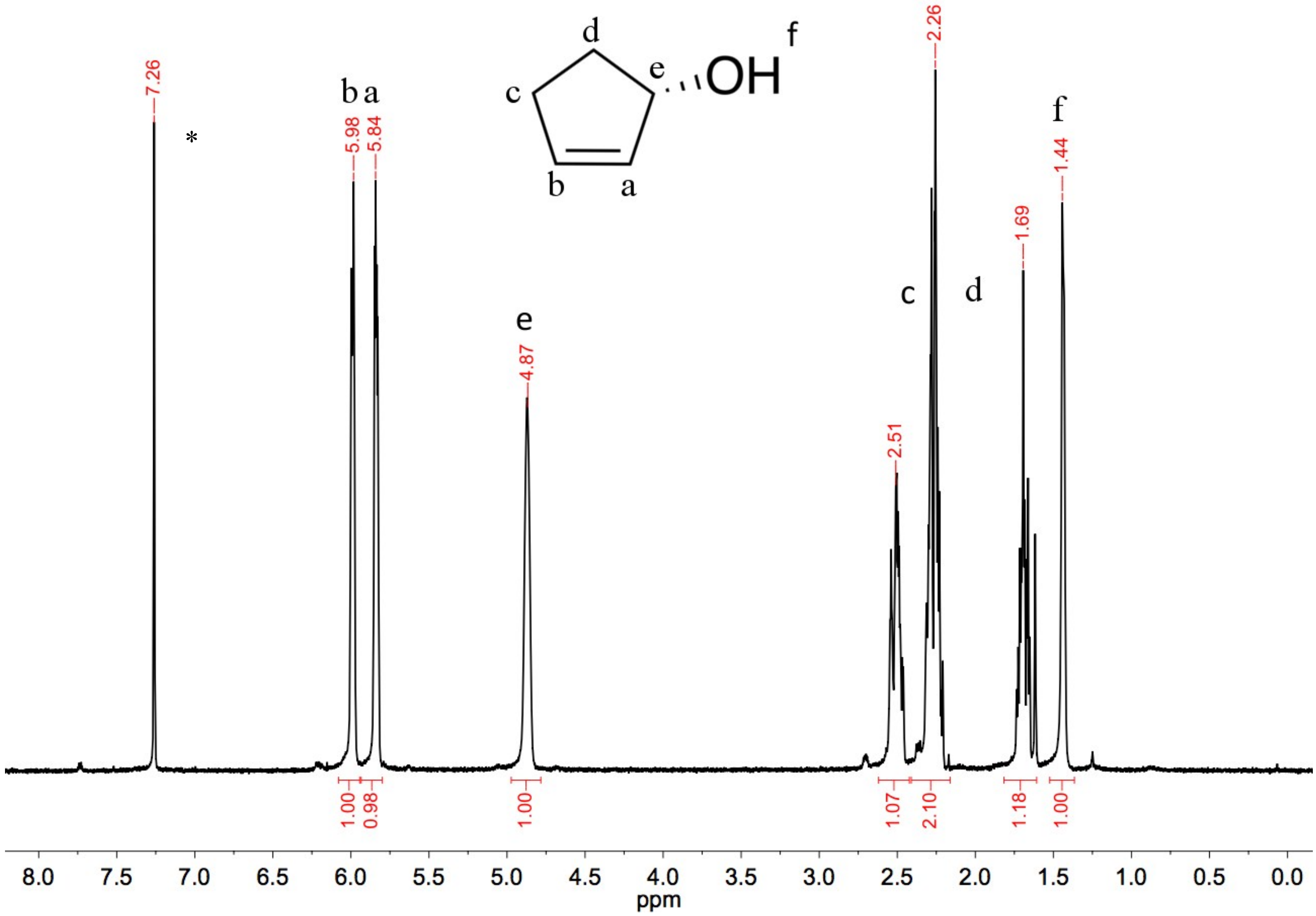

Figure S 17. ^{1}H-NMR spectrum of (*S*)-1 (in *$CDCl_3$, 400 MHz)

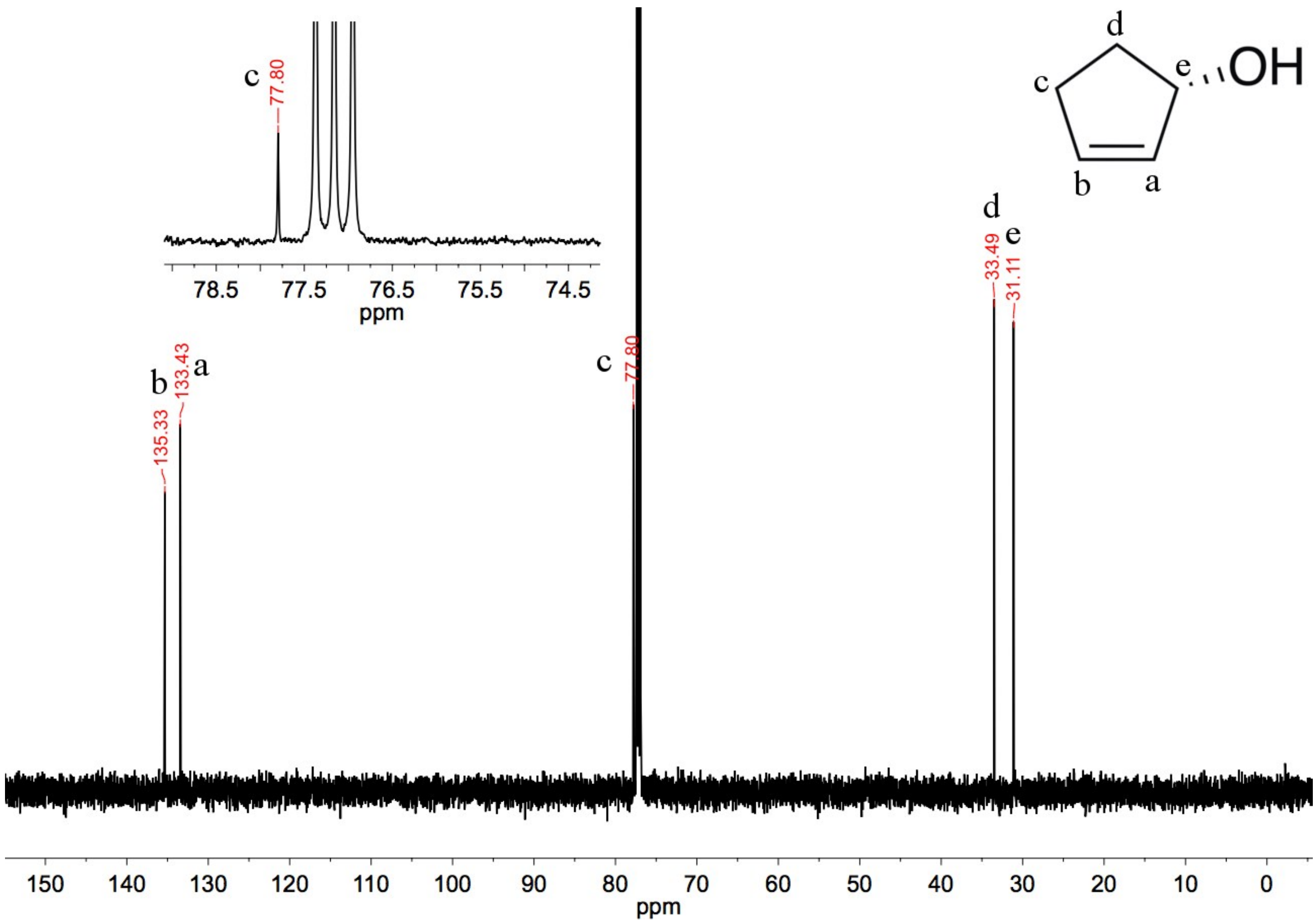

Figure S 18. ^{13}C NMR spectrum of (*S*)-1 (in $CDCl_3$, 150 MHz)

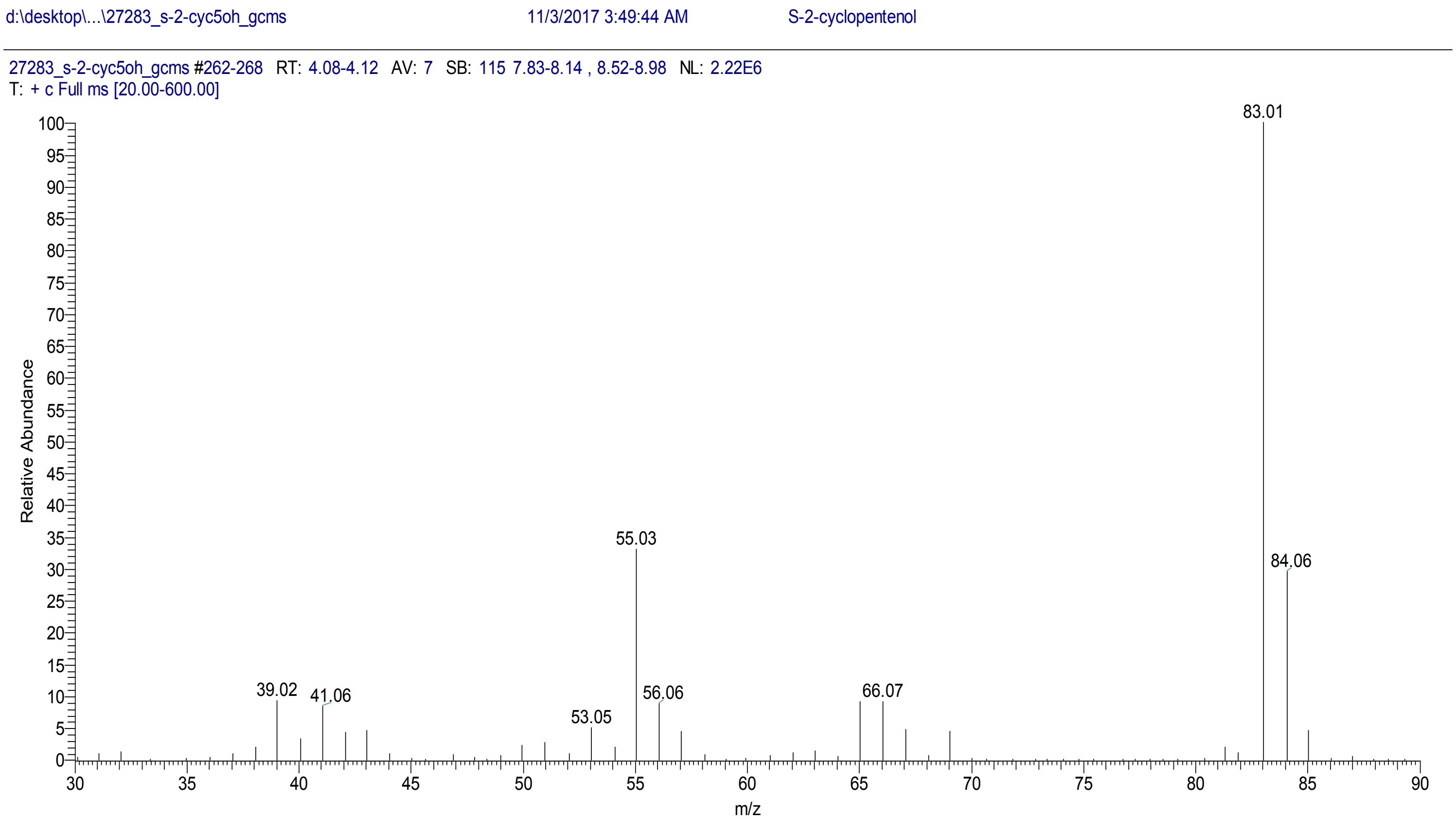

Figure S19: The mass spectrum at RT 4.08-4.12 min for (*S*)-1. The molecular peak is observed at *m/z* 84.06.

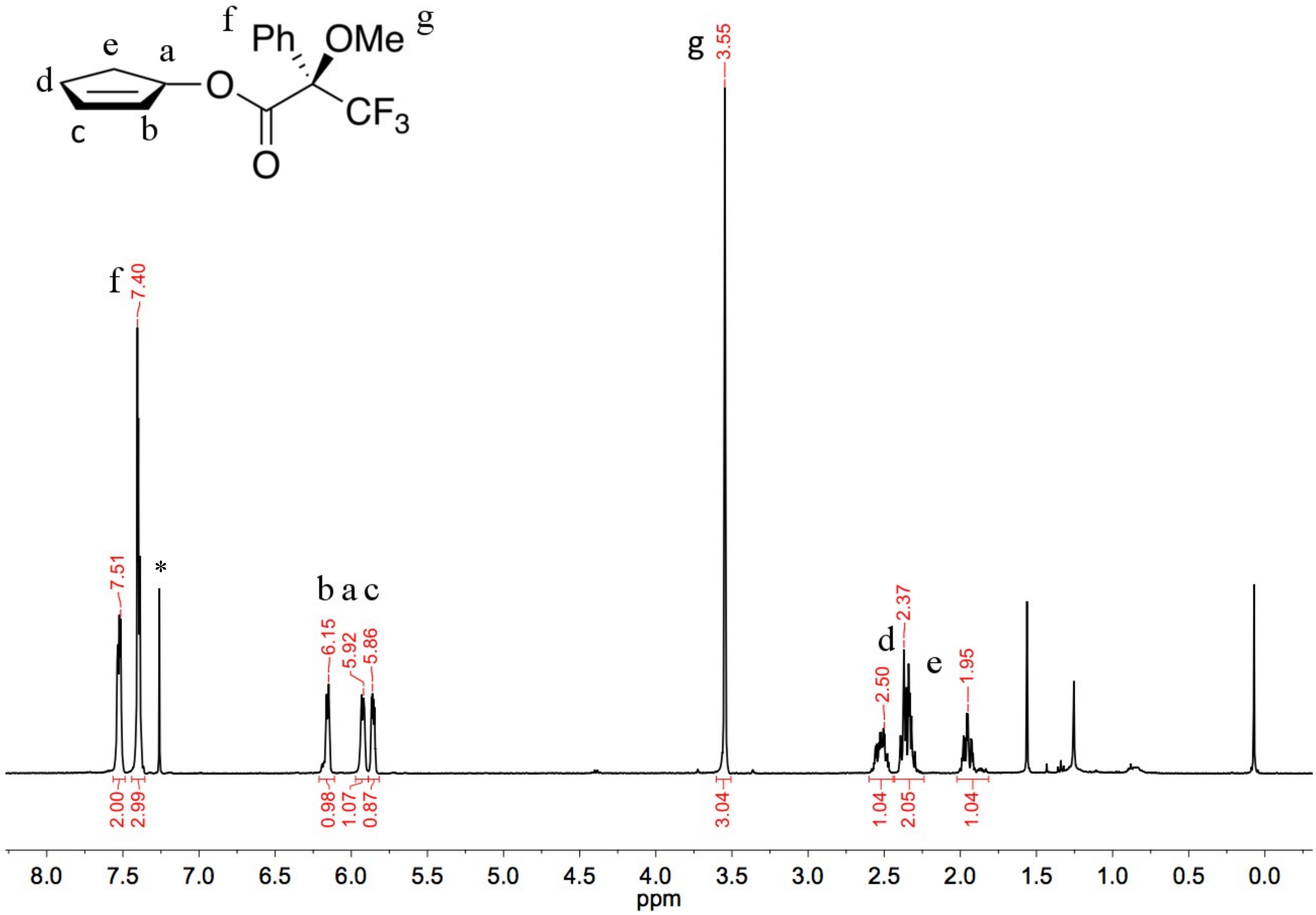

Figure S 20. [1]H-NMR spectrum of (*S*)-2-MTPACP ester (in *$CDCl_3$, 400 MHz).

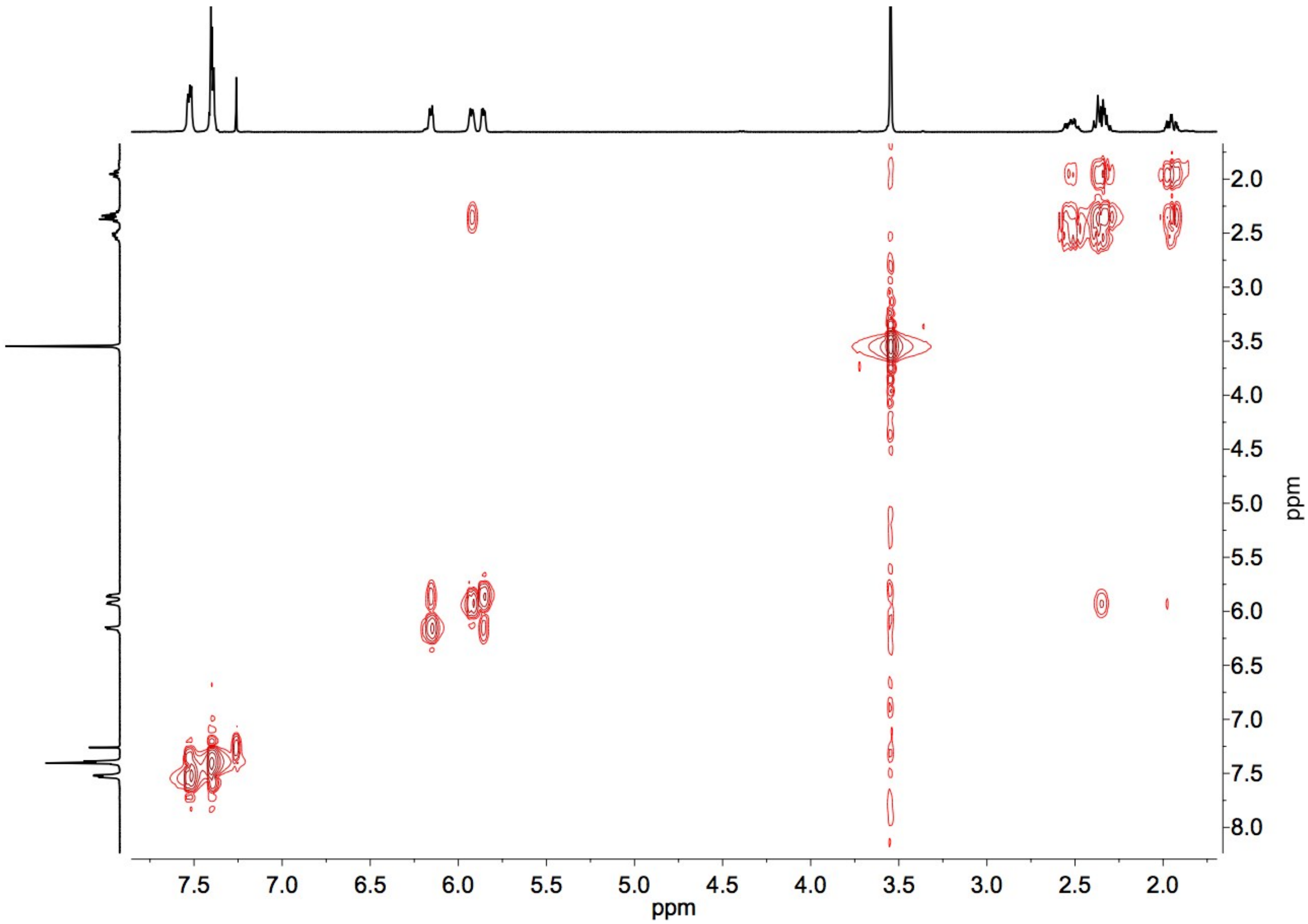

Figure S21. ^1H-^1H COSY spectrum of (*S*)-2-MTPACP ester, (in $CDCl_3$, 400 MHz,).

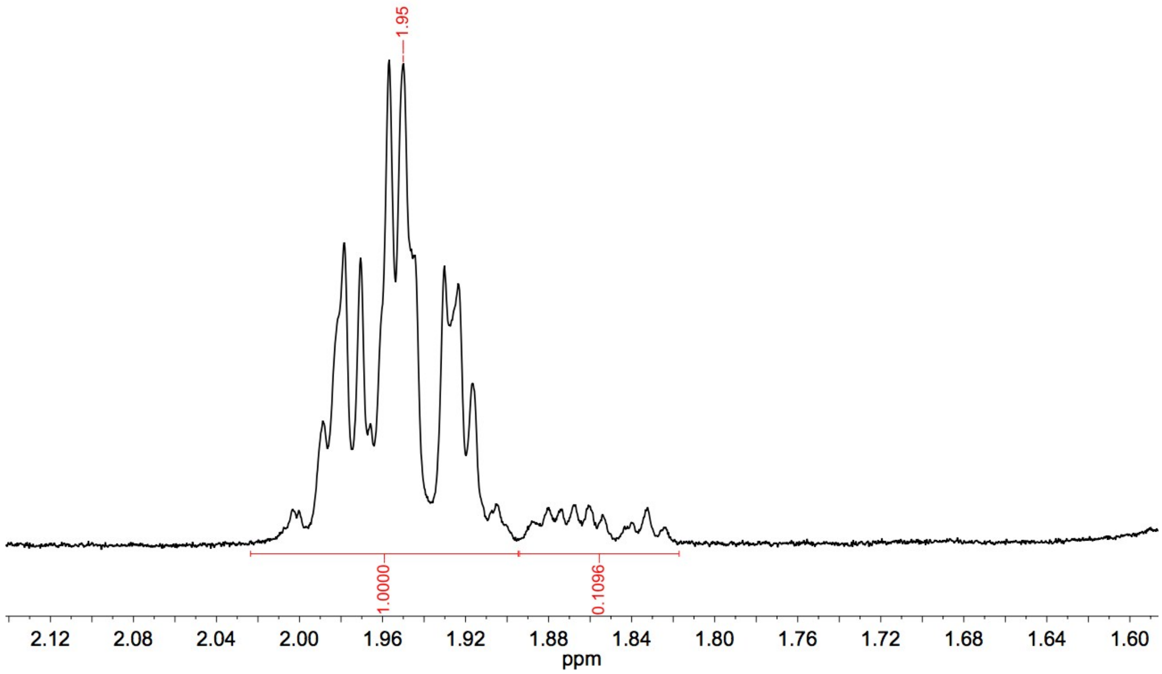

Figure S 22. [1]H-NMR of (*S*)-2-MTPACP ester (in $CDCl_3$, 400 MHz,).

$$\%\ ee = \frac{area\ major}{(area\ major + area\ minor)} * 100 = 90.1\ \%\ ee$$

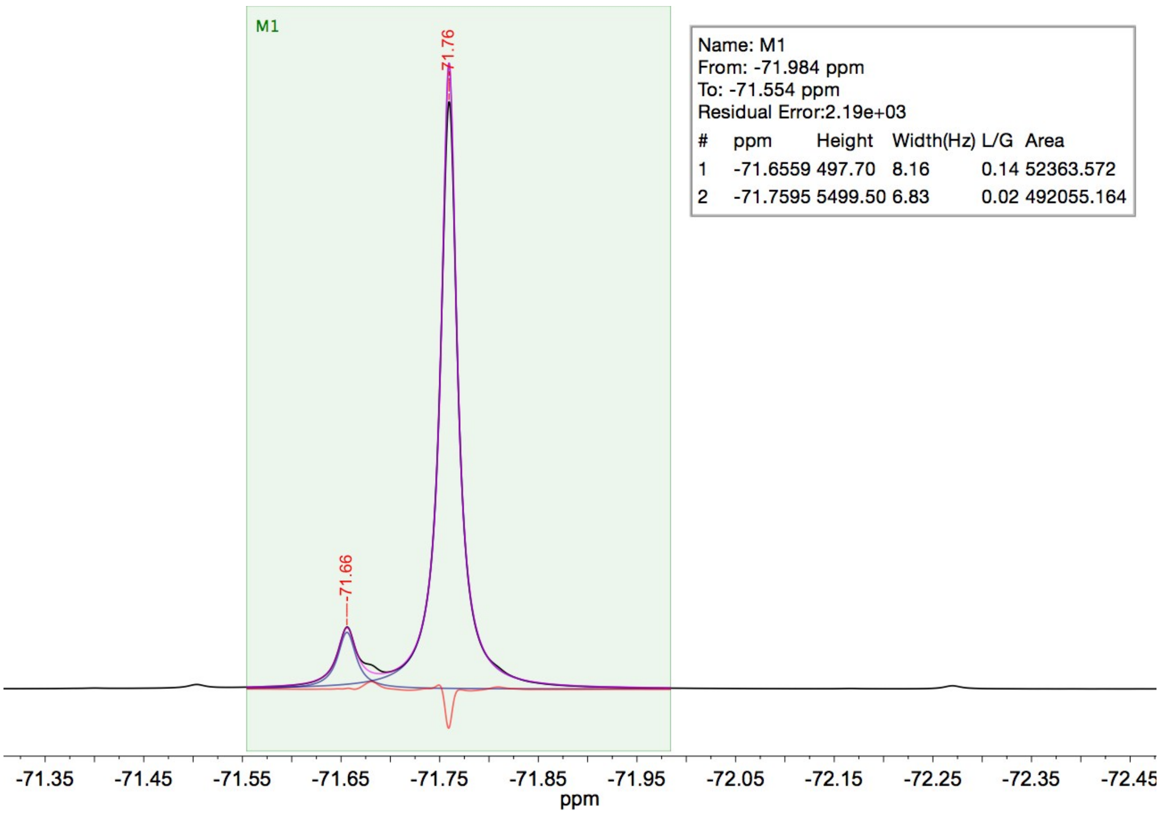

Figure S 23. ^{19}F NMR spectrum of (*S*)-2-MTPACP ester (in $CDCl_3$, 376.5 MHz,). Deconvolution of the peaks were used to determine the integration of the two peaks. $\% \, ee = \frac{area\ major}{(area\ major + area\ min)} * 100 = 90.4\ \%\ ee$

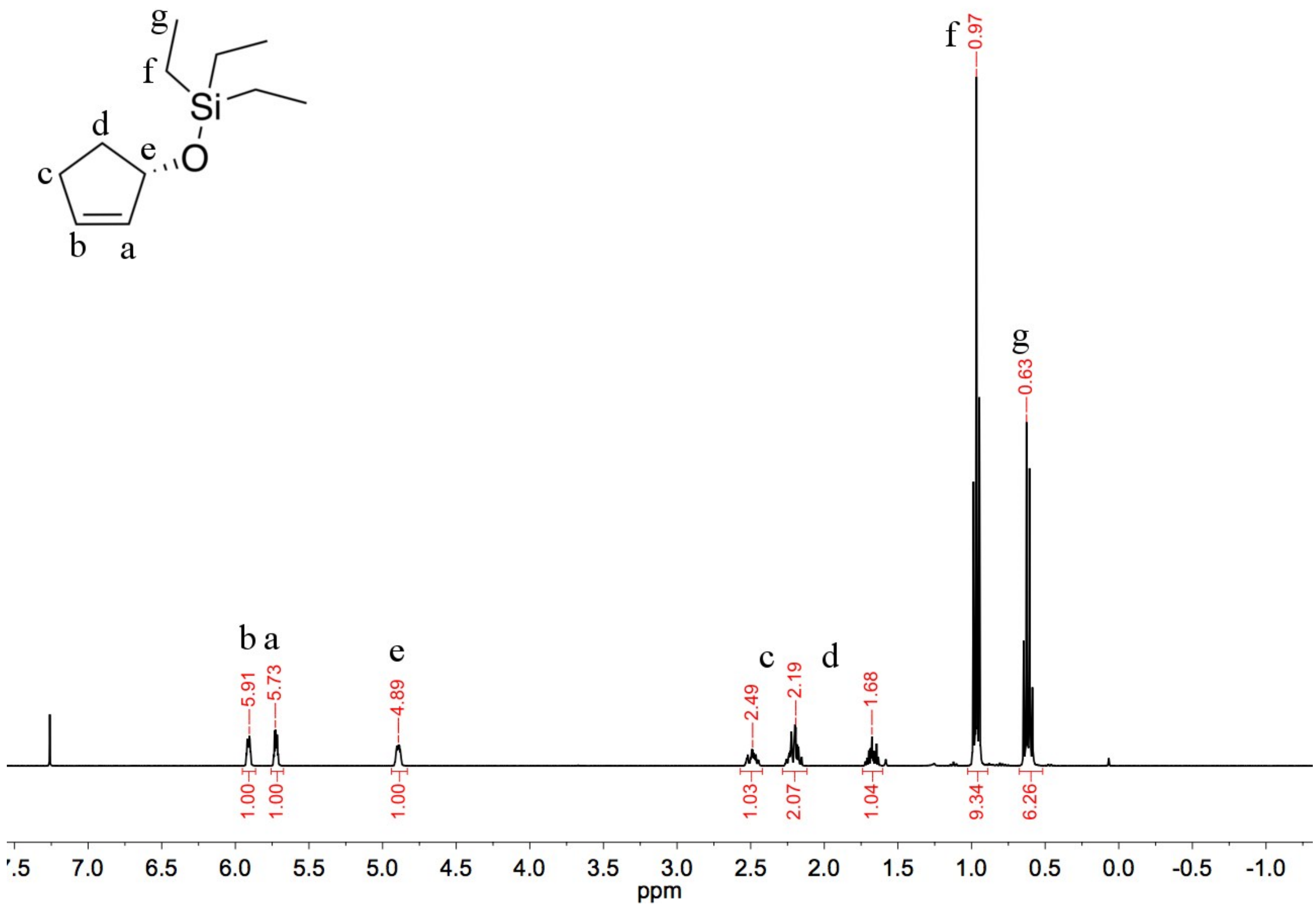

Figure S 24. ^{1}H NMR spectrum of (*S*)-3 (in *CDCl3, 400 MHz).

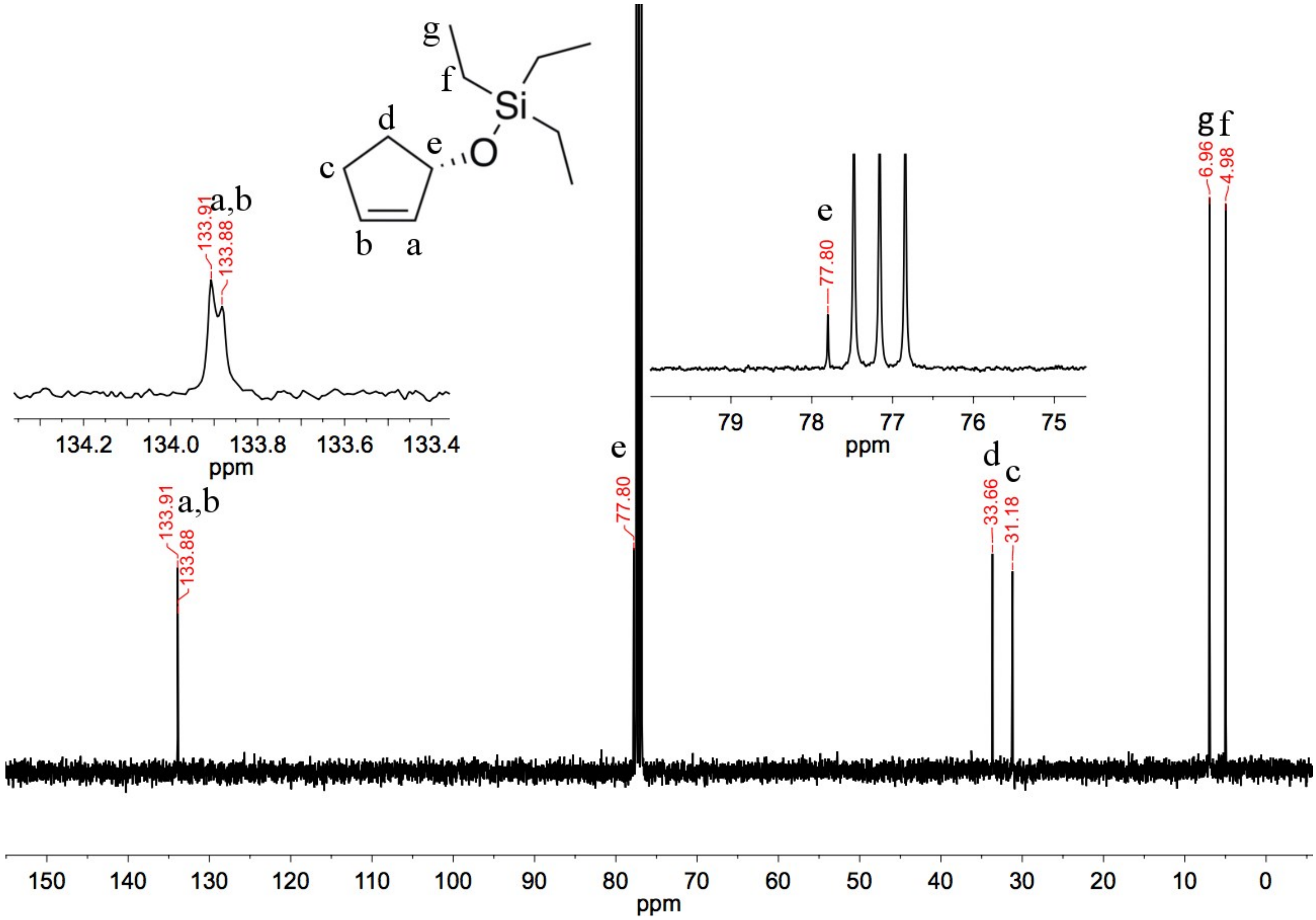

Figure S 25. ^{13}C NMR of (*S*)-3 (in CDCl3, 100 MHz)

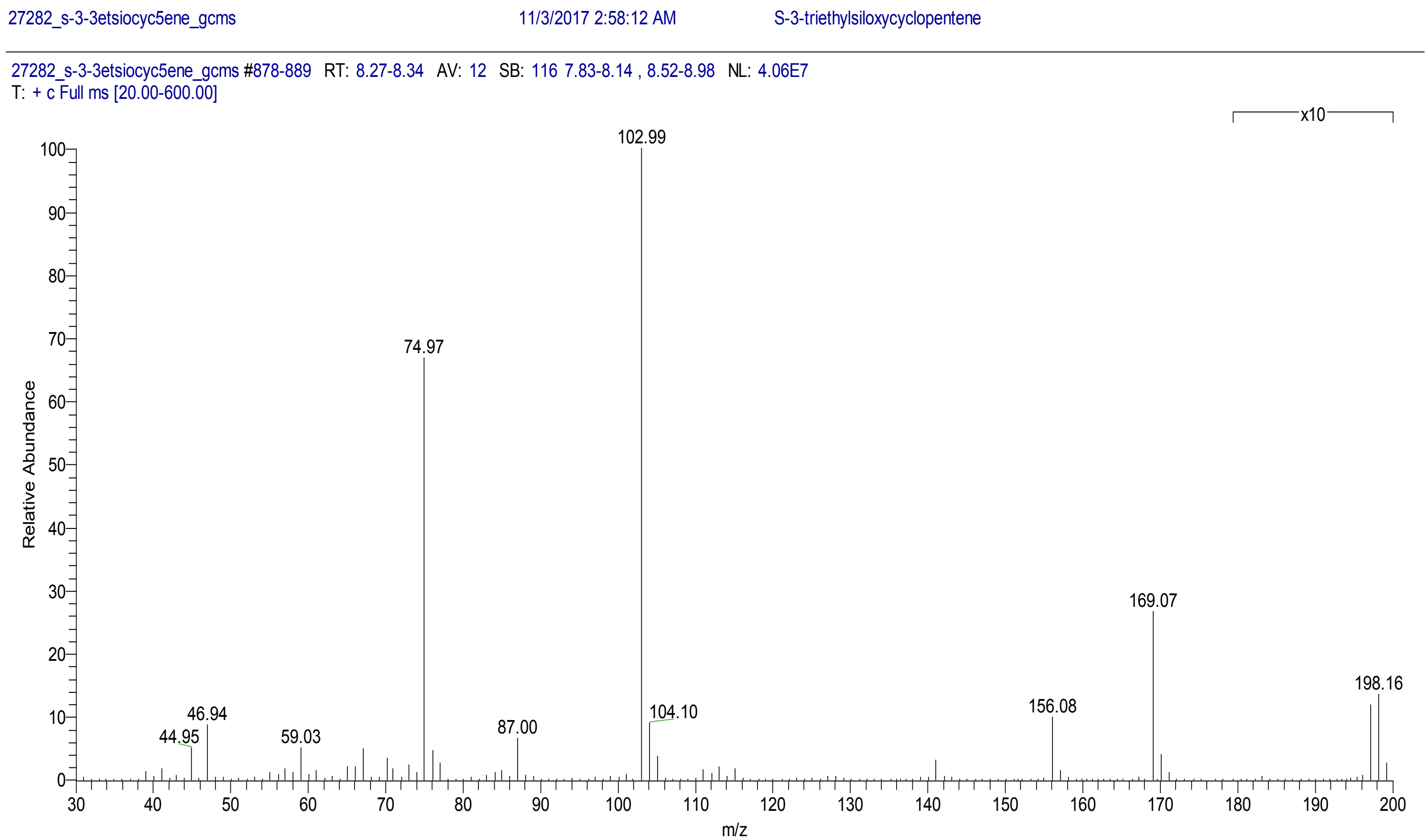

Figure S 26: The mass spectrum at RT 8.27-8.34 min of (*S*)-3. The molecular peak is observed at *m/z* 198.16.

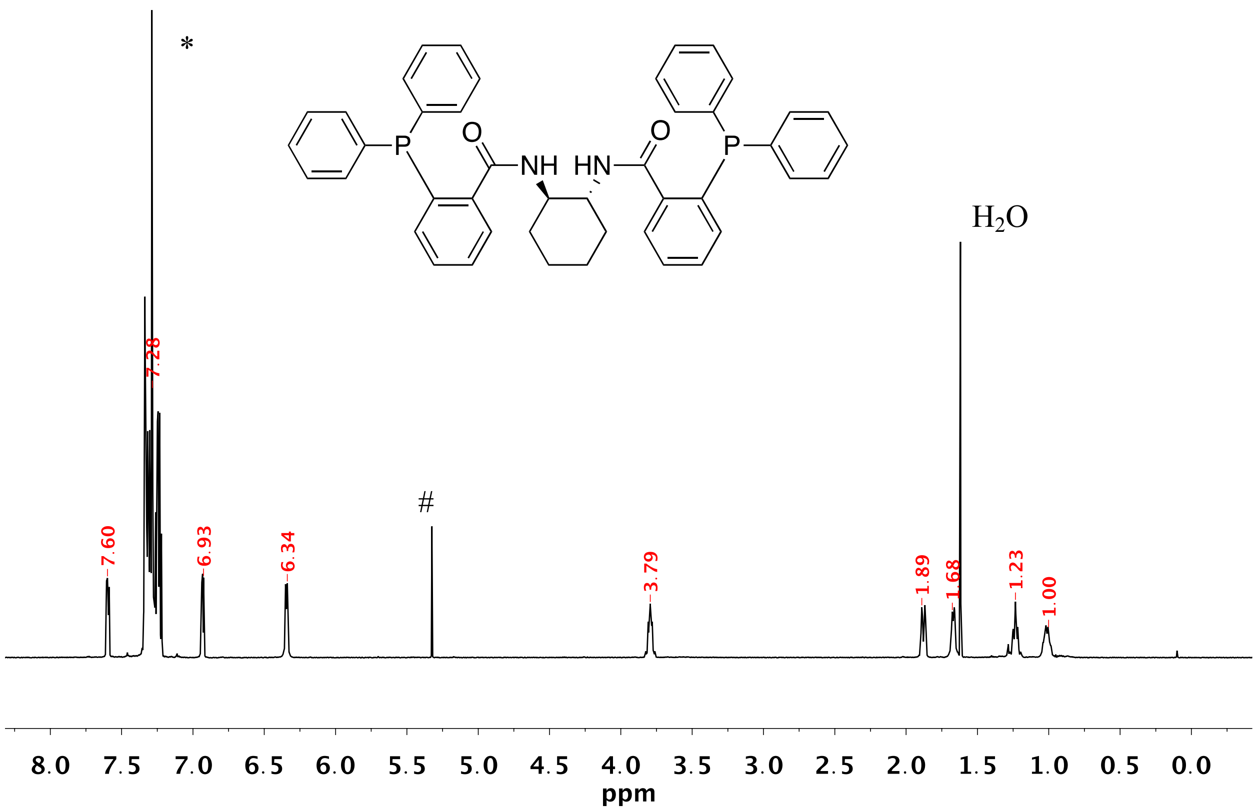

Figure S 27. ^{1}H NMR spectrum of Trost ligand (in *$CDCl_3$, 600 MHz) # DCM

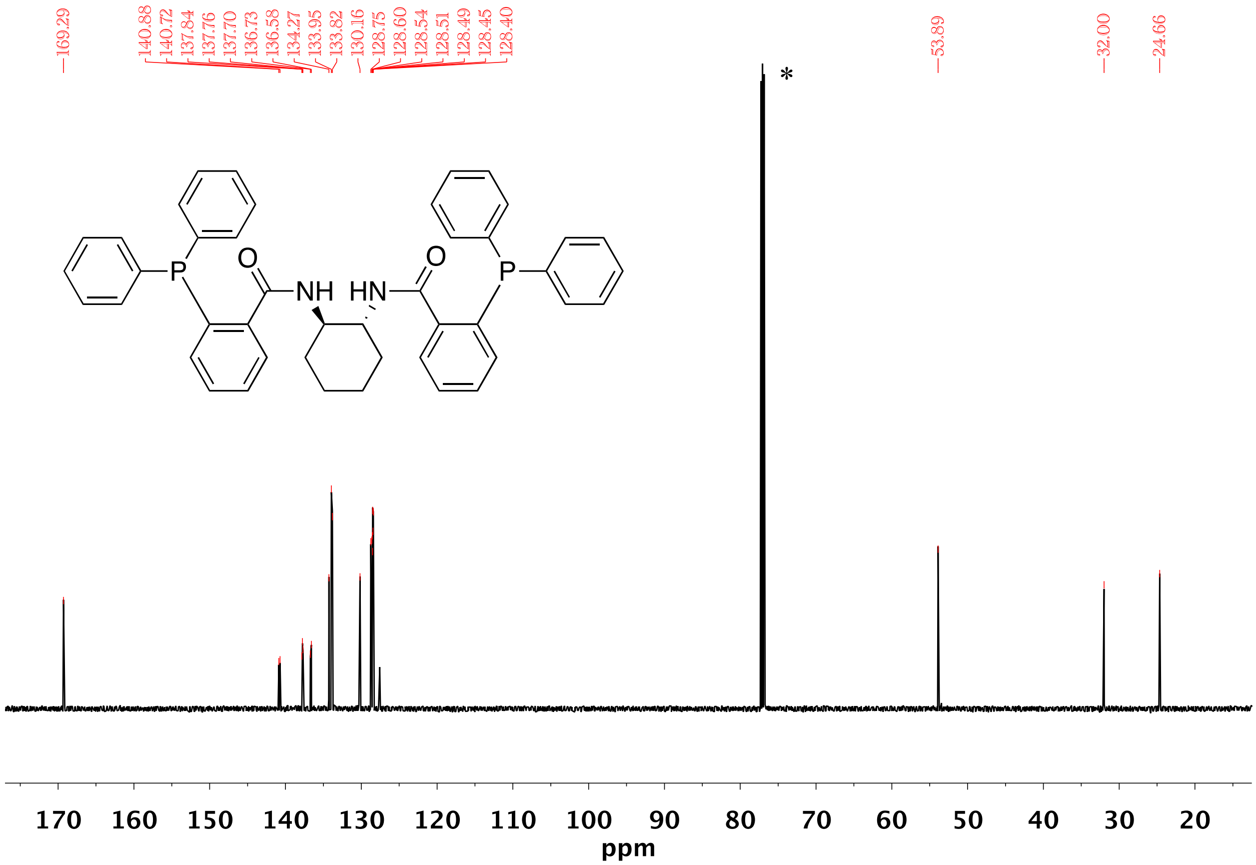

Figure S 28. ^{13}C NMR spectra of the TROST Ligand (in $CDCl_3$, 150 MHz)

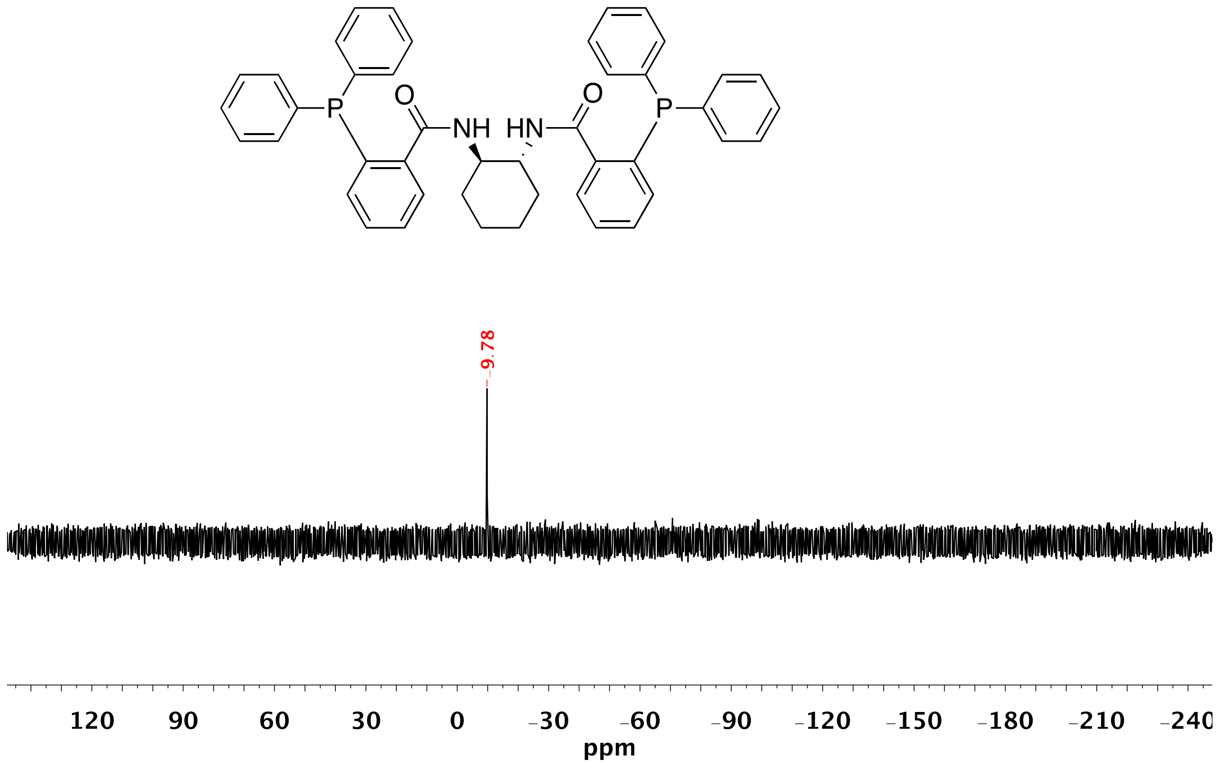

Figure S 29. ^{31}P NMR spectrum of Trost ligand (in $CDCl_3$, 243 MHz)

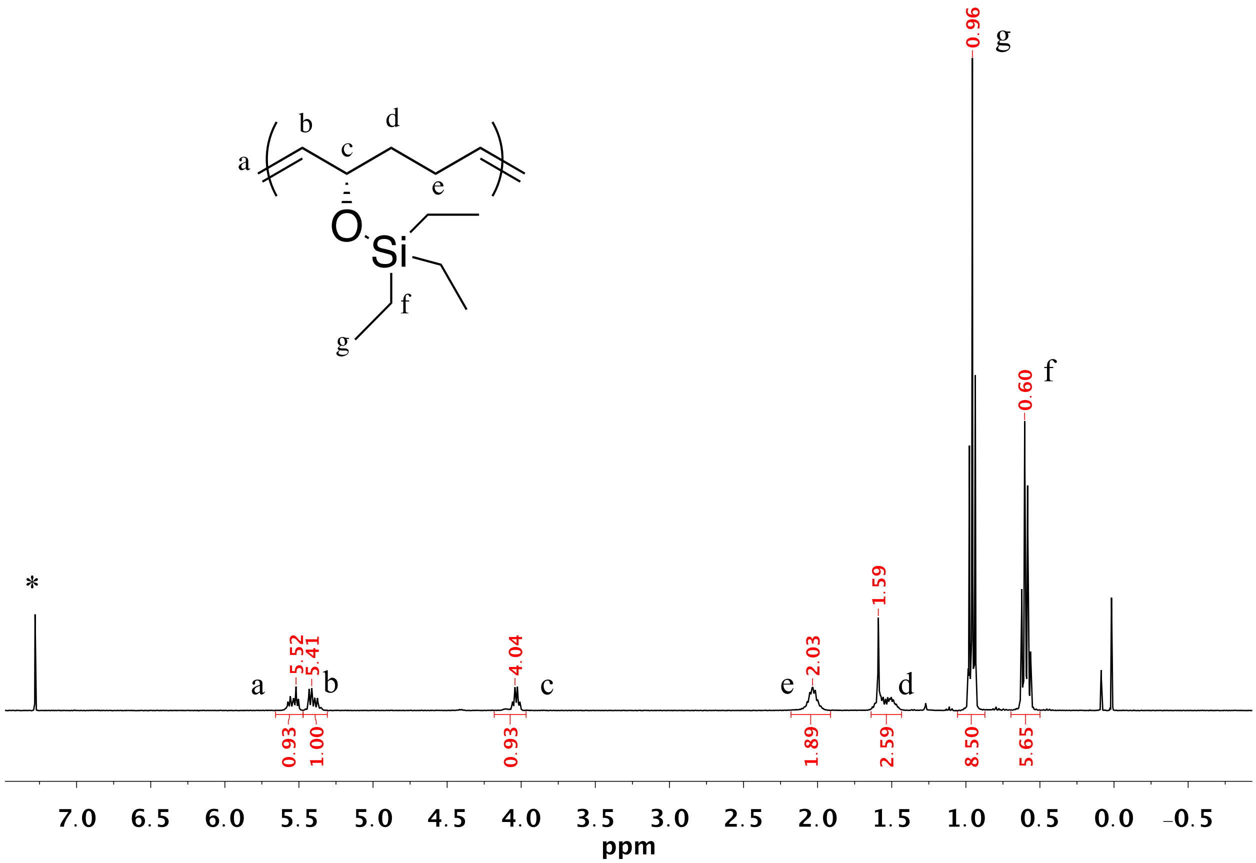

Figure S 30. ^{1}H NMR spectrum of Poly[(*S*)-3], (in *$CDCl_3$, 400 MHz)

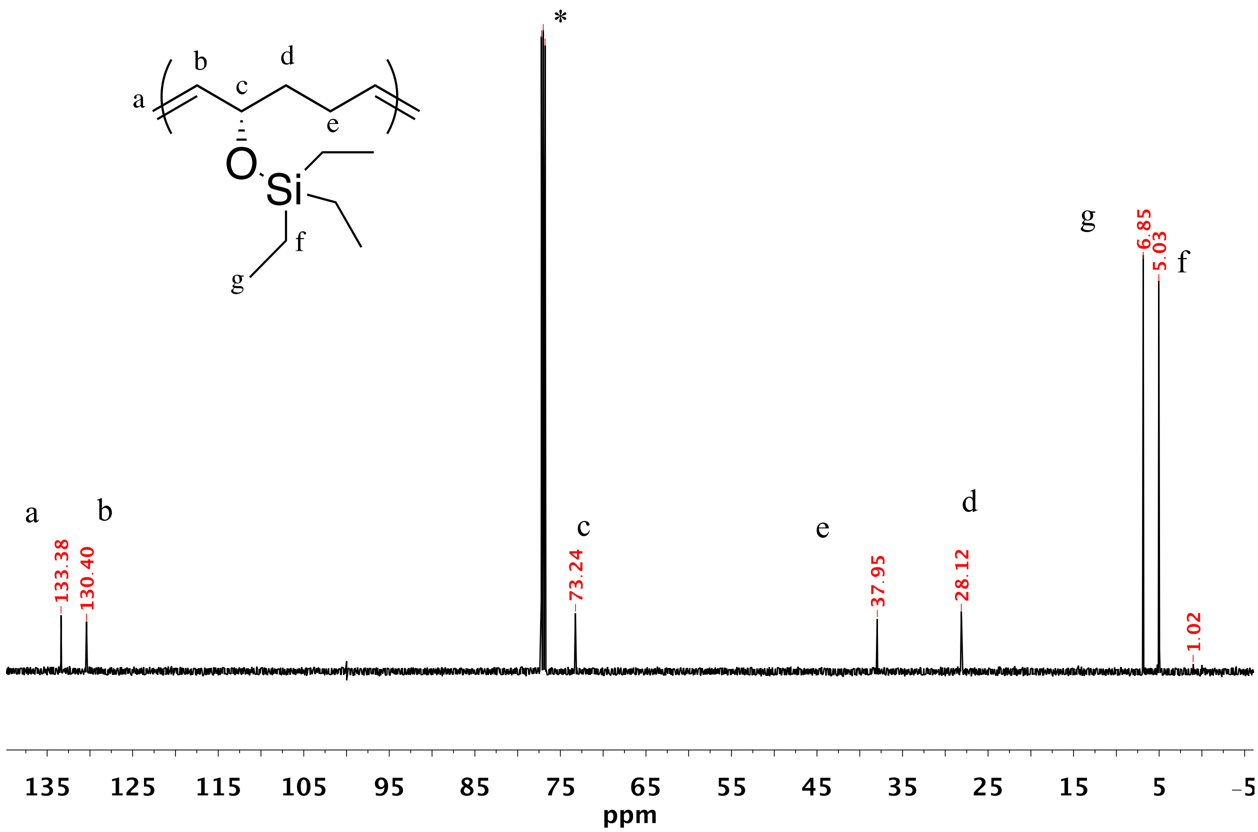

Figure S 31. ^{13}C NMR spectrum of Poly[(*S*)-3], (in *$CDCl_3$, 150 MHz)

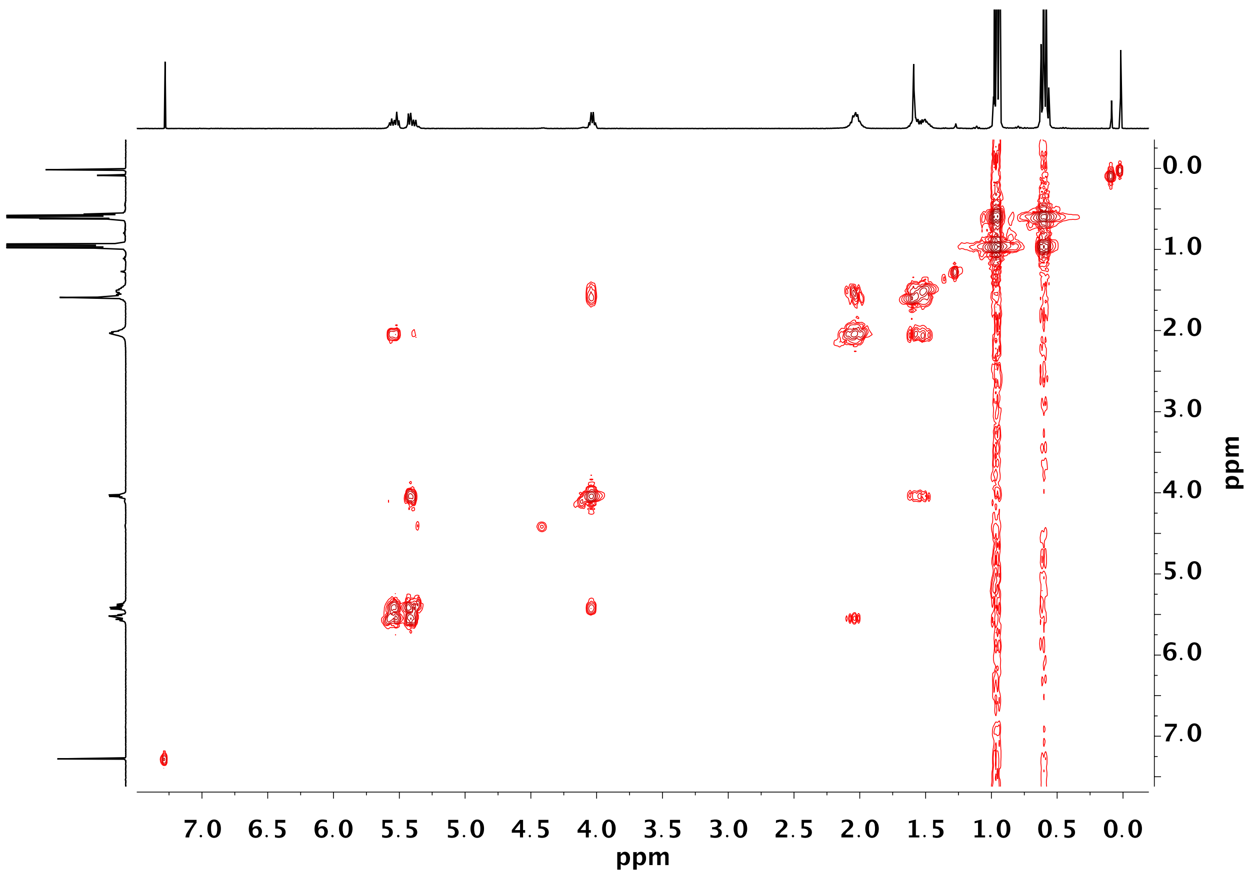

Figure S 32. ^1H-^1H COSY spectrum of Poly[(*S*)-3] ($CDCl_3$, 150 MHz)

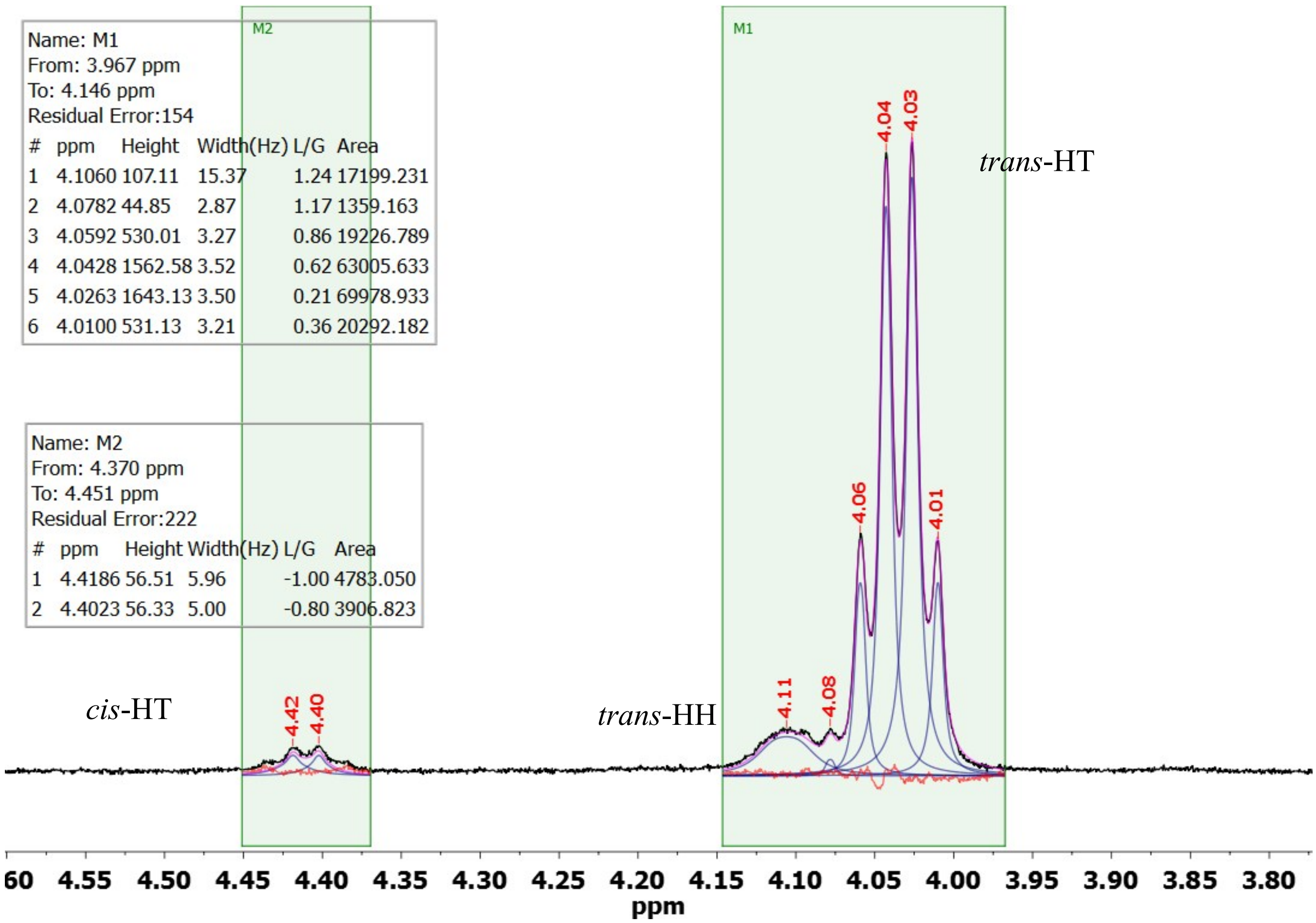

Figure S 33. ^{1}H-NMR spectrum of Poly[(*S*)-3] ($CDCl_3$, 400 MHz). Deconvolution of the peaks were used to determine the %HT and % trans of the polymer.

$$\% HT = \frac{area\ of\ cis - HT + trans - HT}{total\ area\ cis - HT + trans - HH + trans - HT} * 100 = 91.4\ \%.$$

$$\% trans = \frac{area\ of\ trans - HH + trans - HT}{total\ area\ cis - HT + trans - HH + trans - HT} * 100 = 95.6\ \%$$

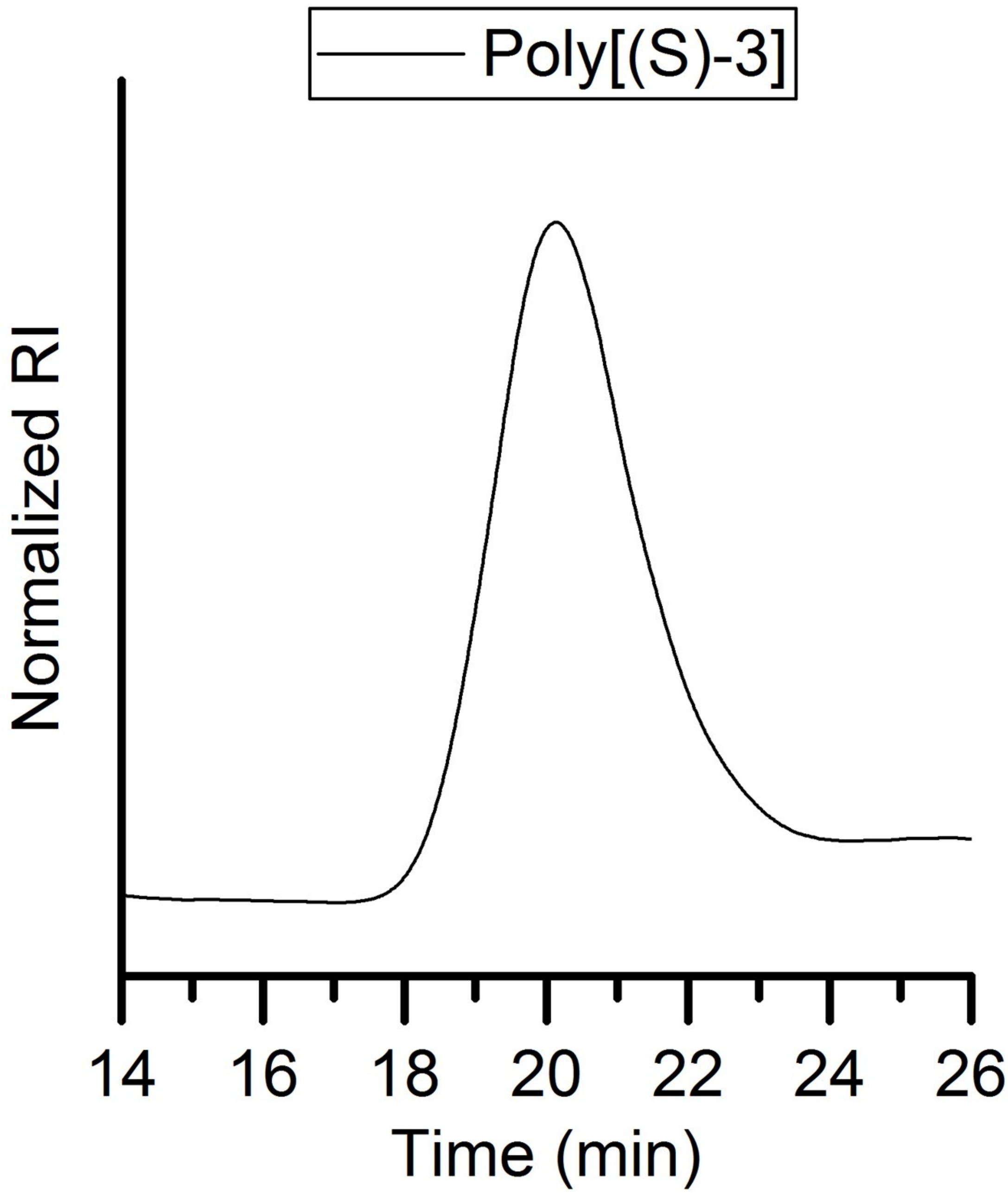

Figure S 34. SEC RI trace of Poly(*S*)-3. (Đ – 2.81, Mn – 30.2 kDa)

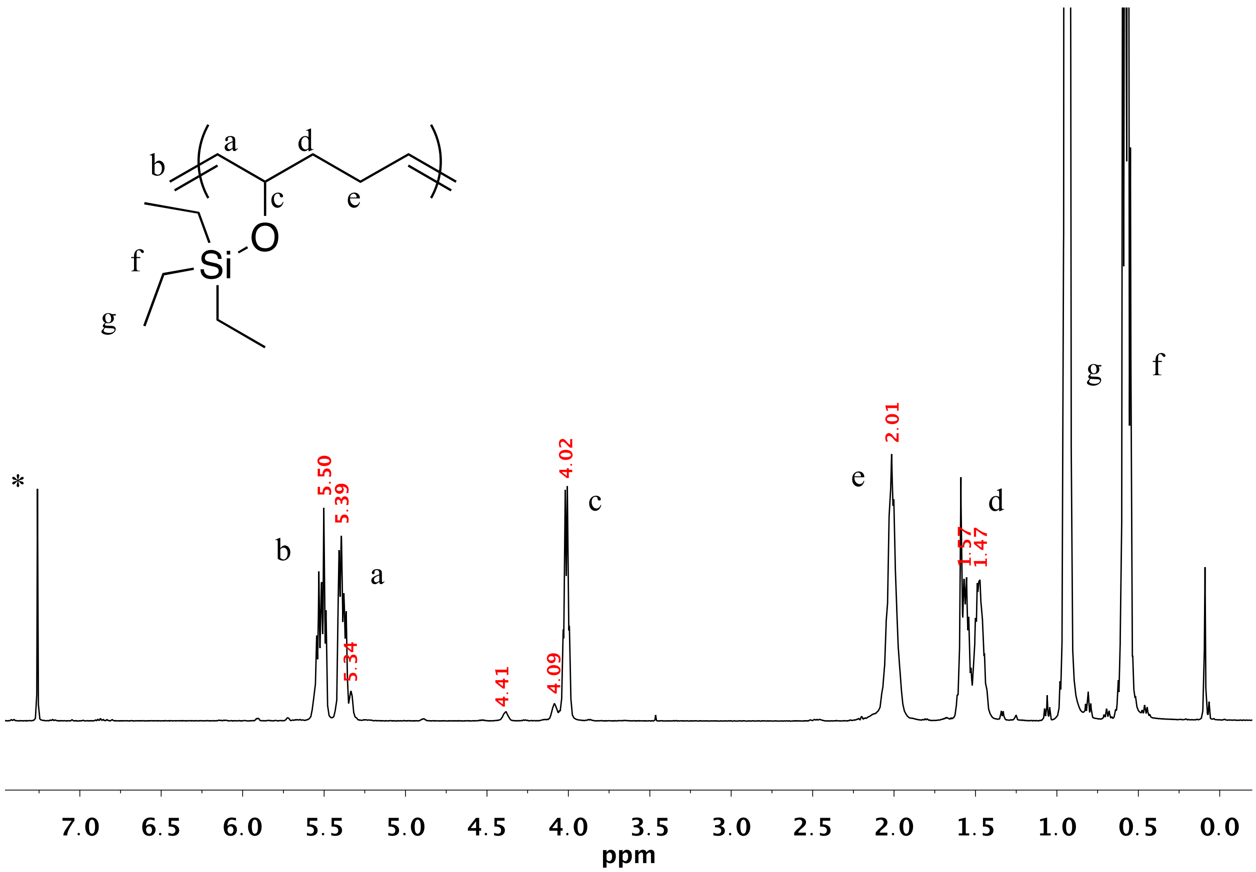

Figure S 35. ^{1}H NMR of spectrum of Poly(*rac*-3), (in *$CDCl_3$, 500 MHz)

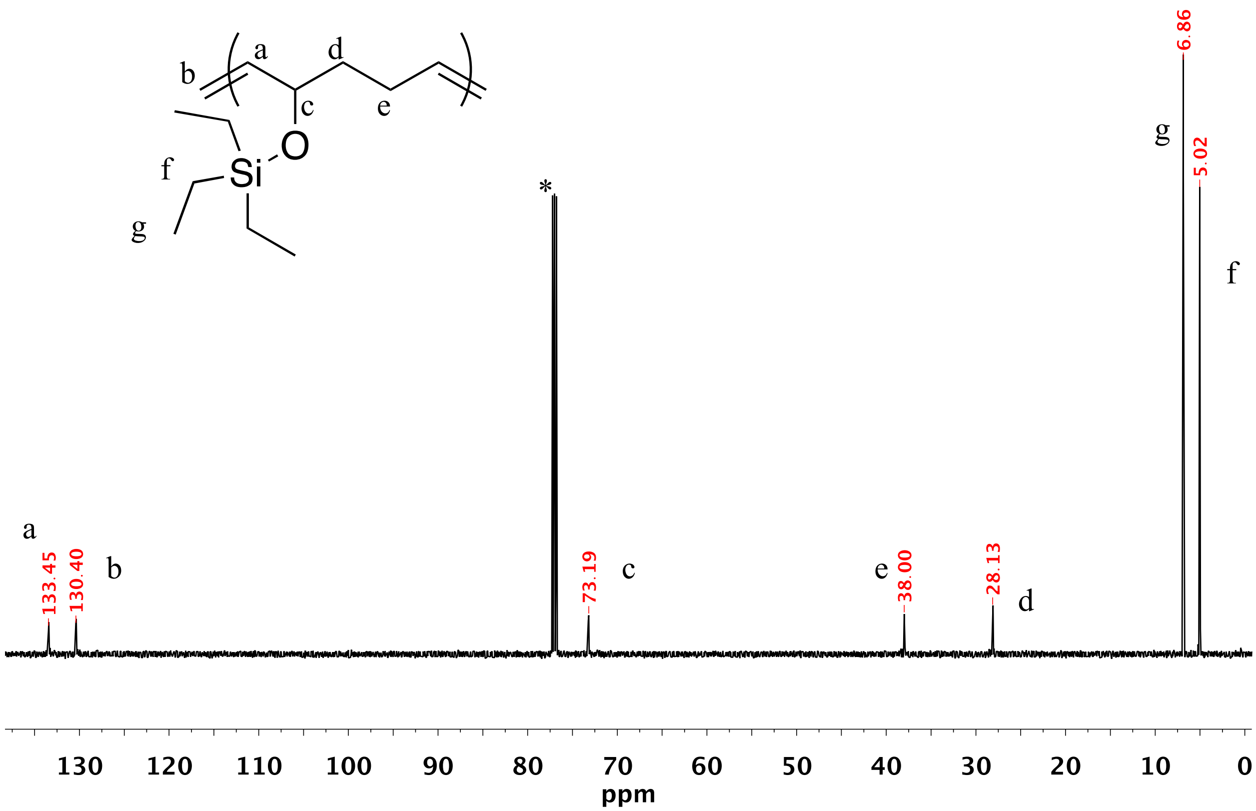

Figure S 36. ^{13}C NMR of spectrum of Poly(*rac*-3), (in *$CDCl_3$, 150 MHz)

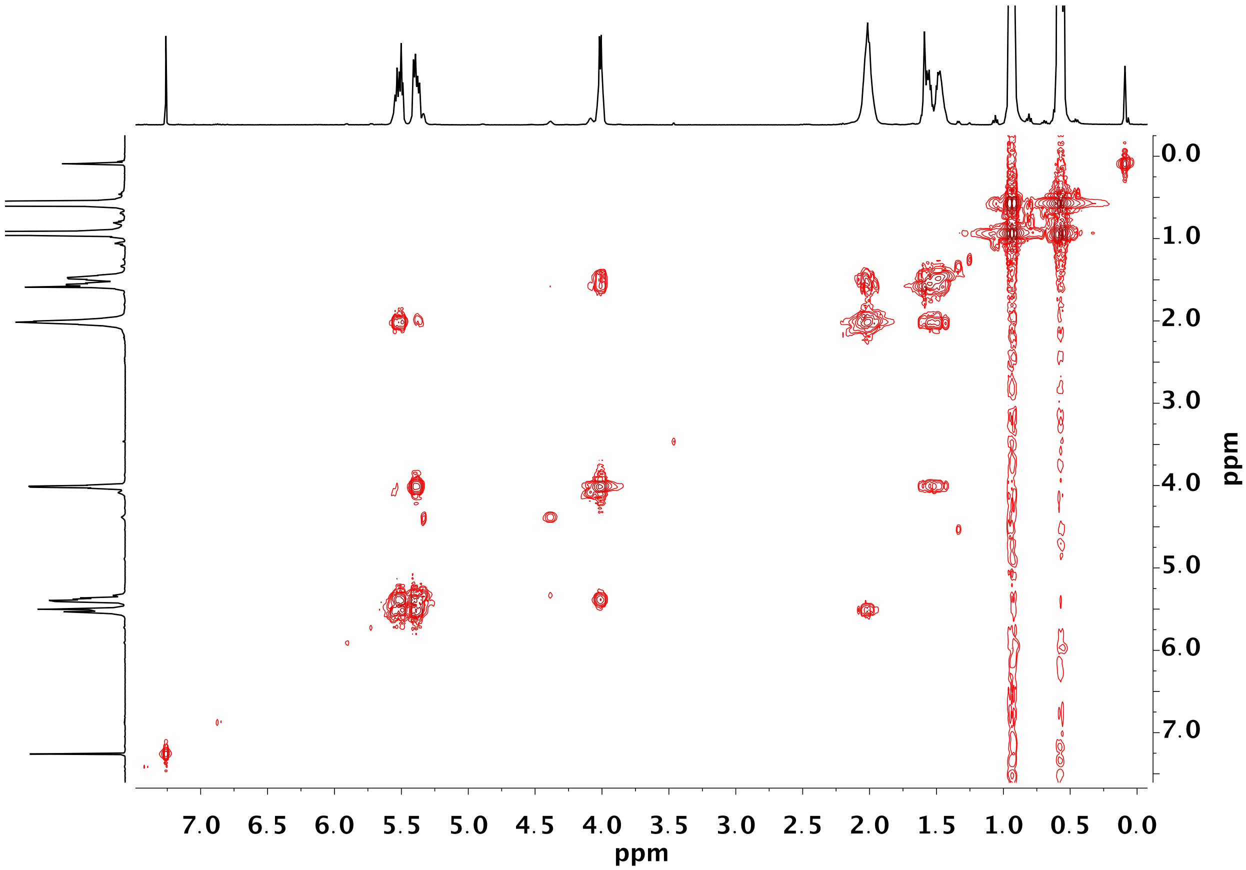

Figure 37. ^{1}H-^{1}H COSY of spectrum of Poly(*rac*-3), (in $CDCl_3$, 500 MHz)

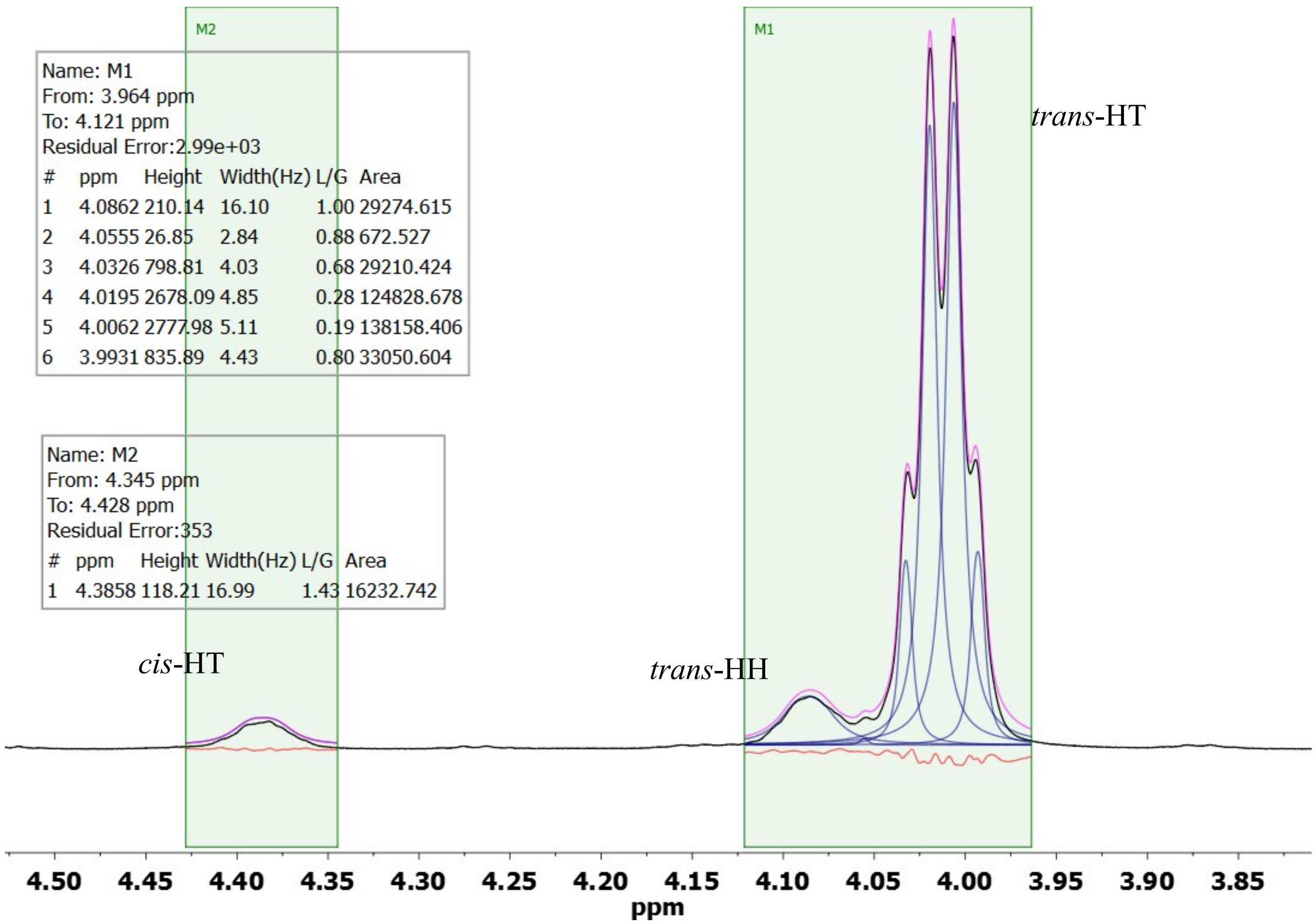

Figure S 38. ^{1}H-NMR spectrum of Poly(*rac*-3) ($CDCl_3$, 400 MHz). ,). Deconvolution of the peaks were used to determine the %HT and % trans of the polymer.

$$\% \, HT = \frac{area \; of \; cis - HT + trans - HT}{total \; area \; cis - HT + trans - HH + trans - HT} * 100 = 92.1 \, \%.$$

$$\% \, trans = \frac{area \; of \; trans - HH + trans - HT}{total \; area \; cis - HT + trans - HH + trans - HT} * 100 = 95.6 \, \%.$$

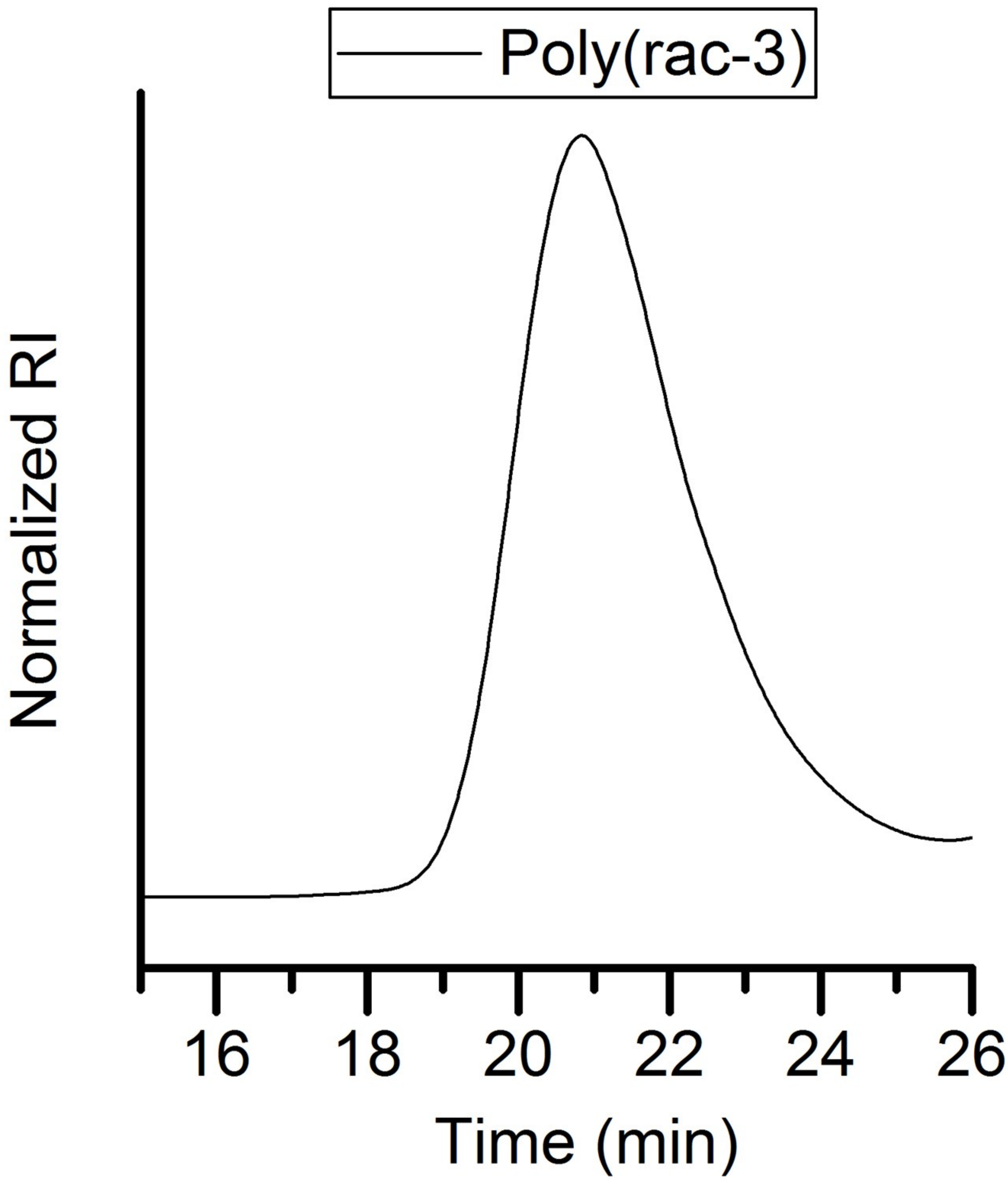

Figure S 39. SEC RI trace of Poly(*rac*-3). (Đ – 2.56, Mn – 22.3 kDa)

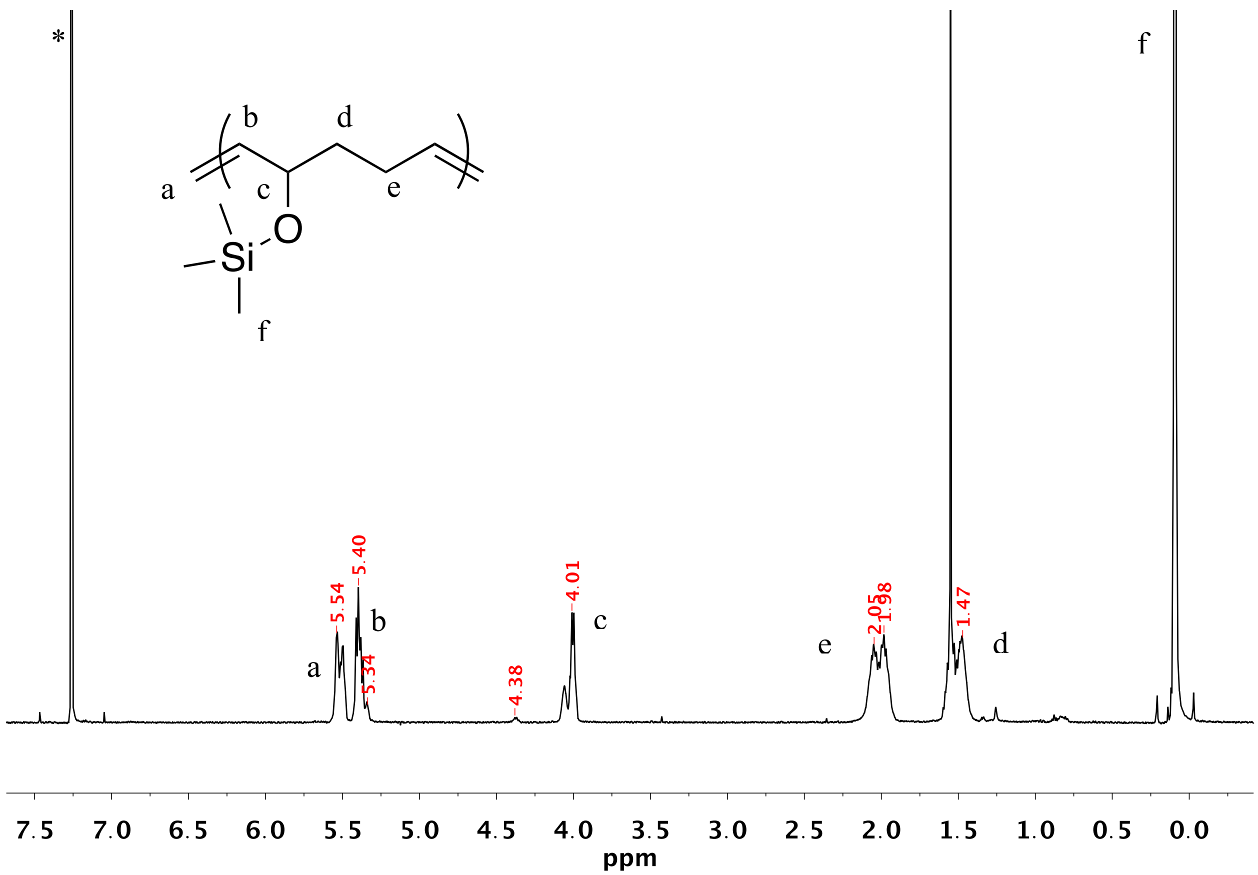

Figure S 40. ^{1}H NMR spectrum of Poly(*rac*-2), (in *$CDCl_3$, 500 MHz)

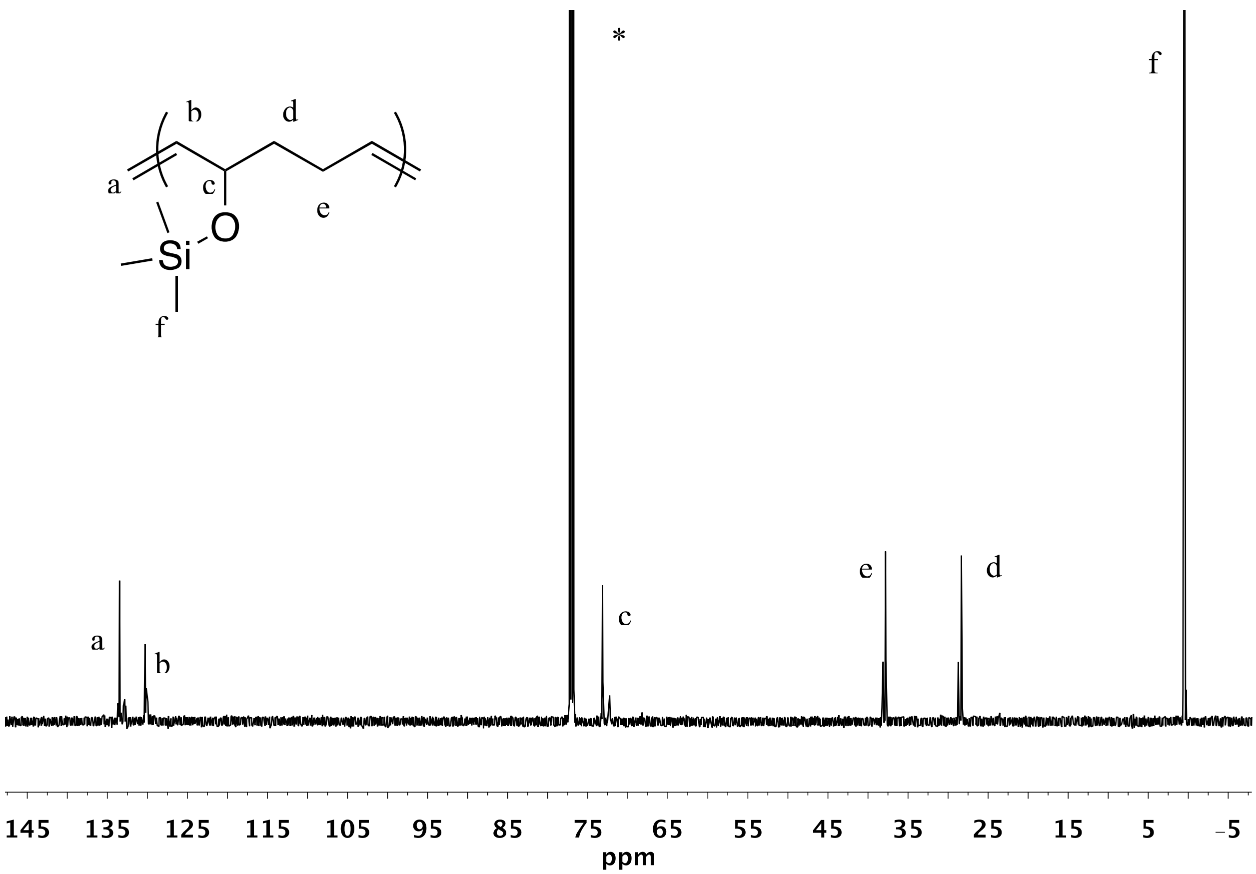

b
d
a
c
e
O
Si
f
*
f
e
d
c
a
b
145
135
125
115
105
95
85
75
65
55
45
35
25
15
5
-5
ppm

Figure S 41. ^{13}C NMR spectrum of Poly(*rac*-2), (in *$CDCl_3$, 150 MHz)

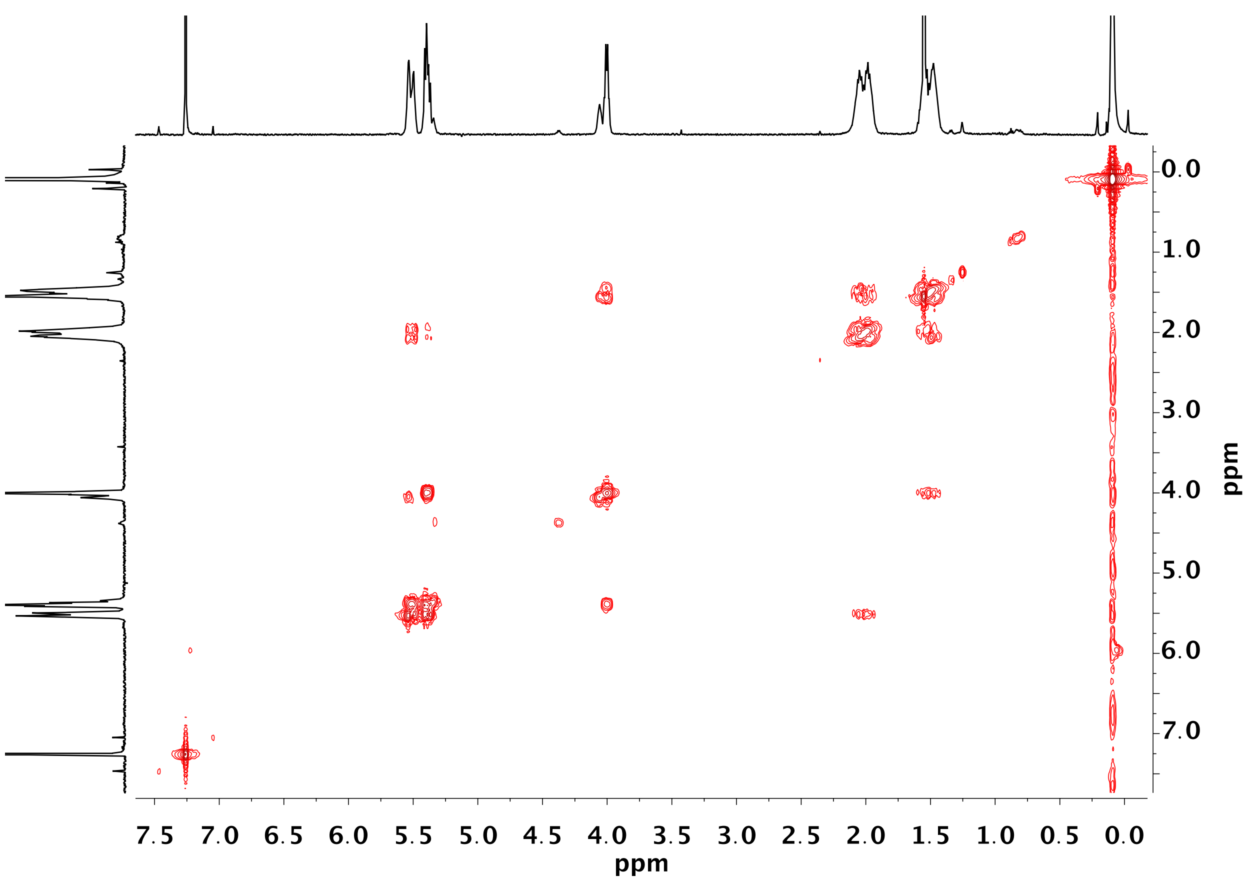

Figure S 42. ^{1}H-^{1}H COSY spectrum of Poly(*rac*-2), (in $CDCl_3$, 500 MHz)

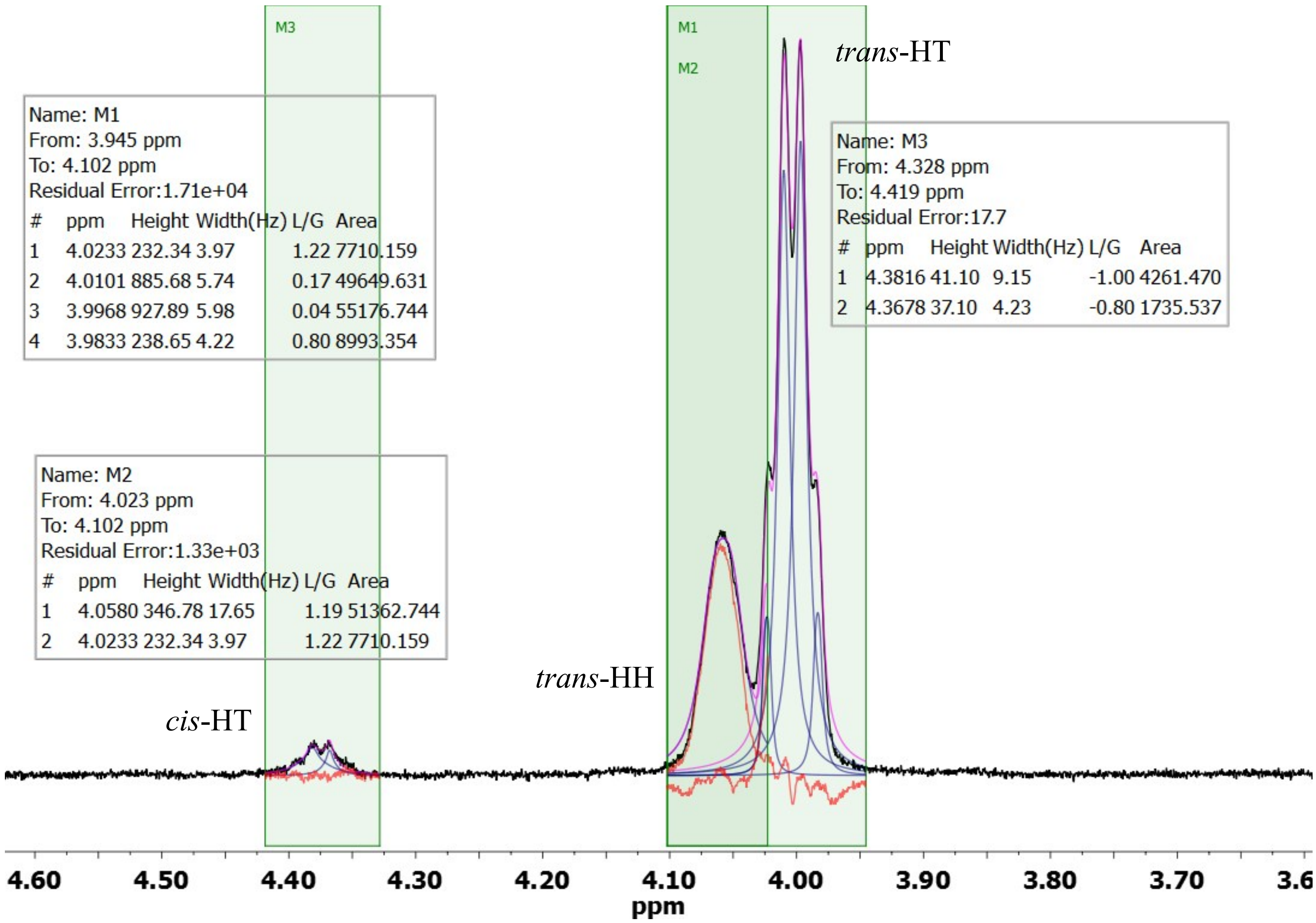

Figure S 43. [1]H-NMR spectrum of Poly(*rac*-2) ($CDCl_3$, 400 MHz). ,). Deconvolution of the peaks were used to determine the %HT and % trans of the polymer.

$$\% \, HT = \frac{area \; of \; cis - HT + trans - HT}{total \; area \; cis - HT + trans - HH + trans - HT} * 100 = 68.3 \, \%.$$

$$\% \, trans = \frac{area \; of \; trans - HH + trans - HT}{total \; area \; cis - HT + trans - HH + trans - HT} * 100 = 94.2 \, \%.$$

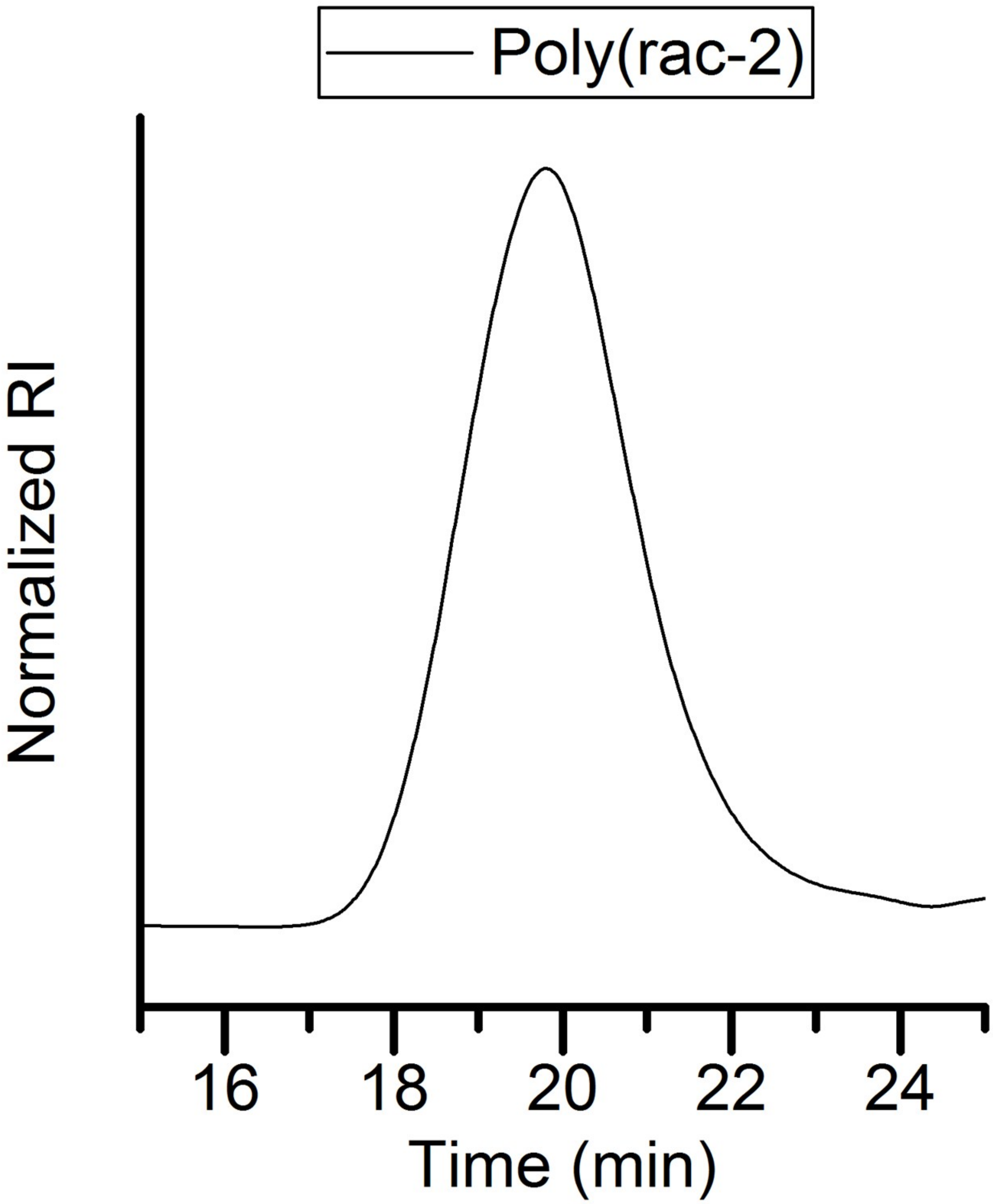

Figure S 44. SEC RI trace of Poly(*rac*-2). (Đ – 2.07, Mn – 41.6 kDa)

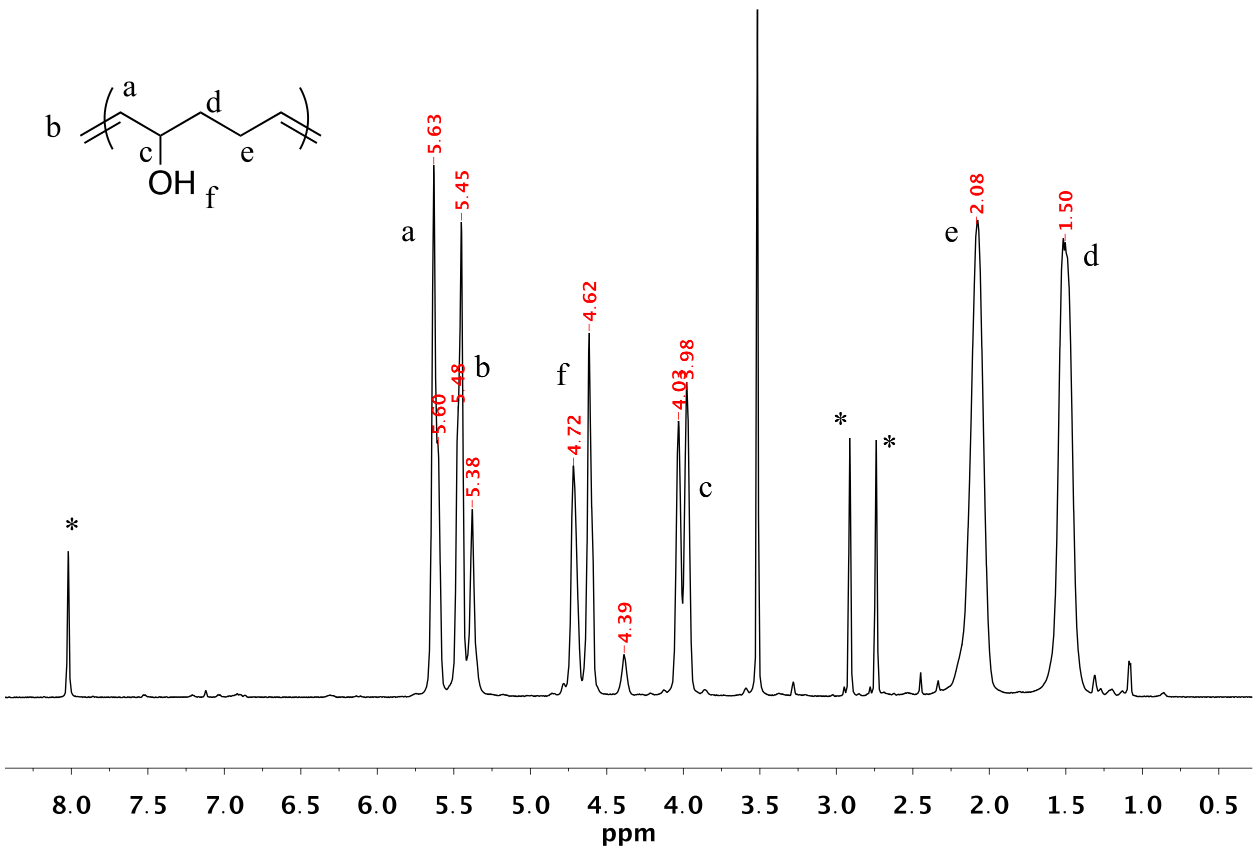

Figure S 45. ^{1}H NMR spectrum of Poly(*rac*-1), (*DMF-d_7, 600 MHz)

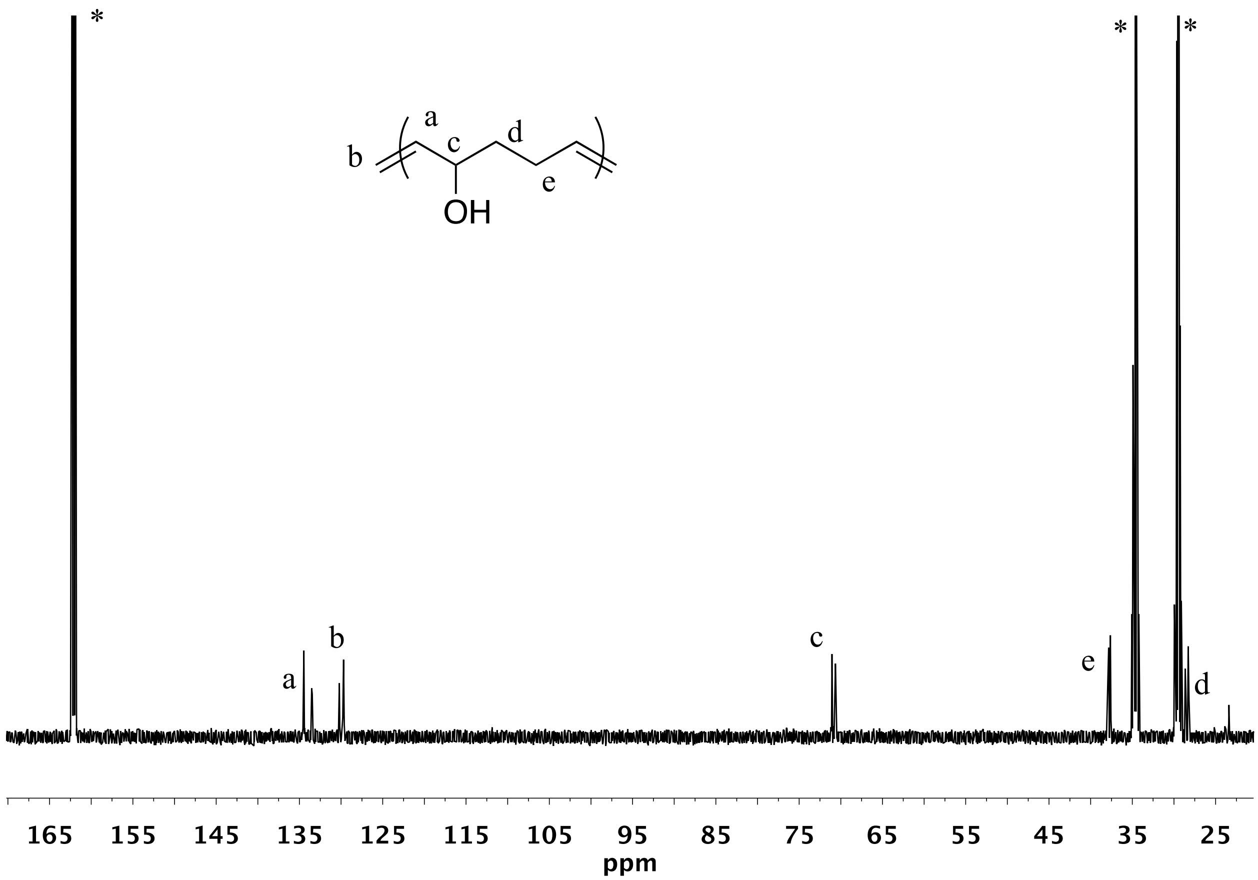

Figure S 46. ^{13}C NMR spectrum of Poly(*rac*-1), (*DMF$_7$, 150 MHz)

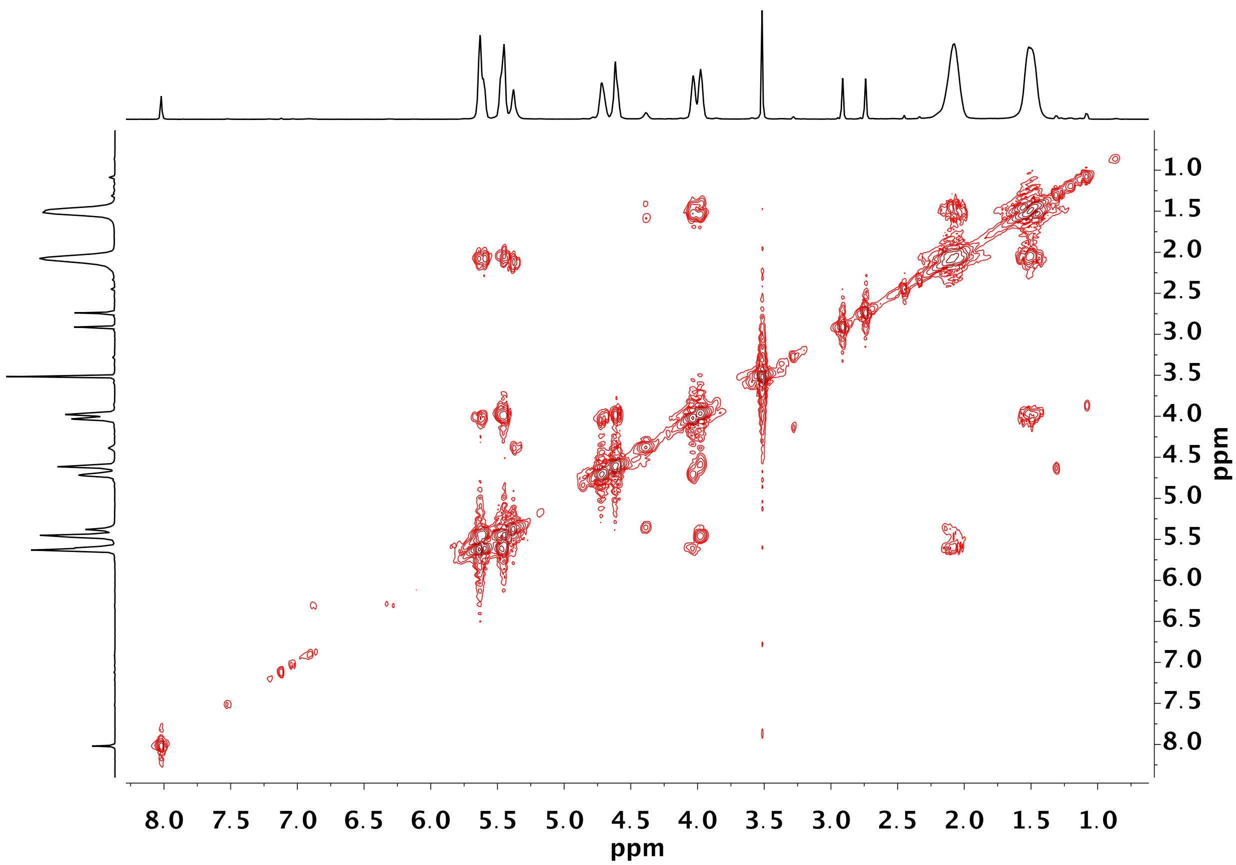

Figure S 47. ^{1}H-^{1}H COSY spectra of Poly(*rac*-1) ($CDCl_3$, 600 MHz)

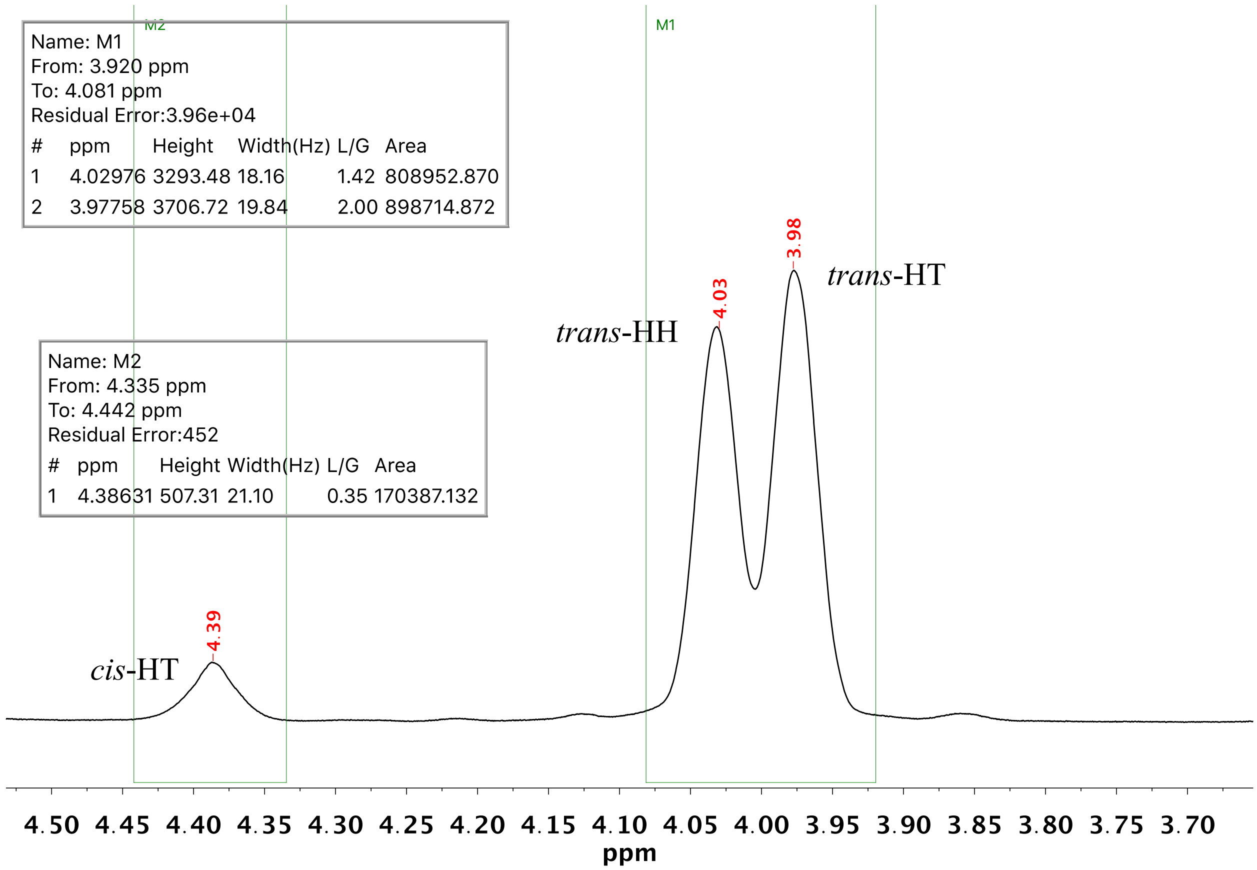

Figure S 48. ^{1}H-NMR spectrum of Poly(*rac*-1) ($CDCl_3$, 400 MHz). Deconvolution of the peaks were used to determine the %HT and % trans of the polymer.

$$\% HT = \frac{area\ of\ cis - HT + trans - HT}{total\ area\ cis - HT + trans - HH + trans - HT} * 100 = 57\ \%.$$

$$\% trans = \frac{area\ of\ trans - HH + trans - HT}{total\ area\ cis - HT + trans - HH + trans - HT} * 100 = 91\ \%.$$

Table S49: Aliquot characterization of Poly(*rac*-3) at 2.5 M with HG2 at -10 °C.

Time (min)	conv[a] %
31.5	4.8
52.33	14.5
90	33.1
116	33.3
157	33.3

[a] Determined by ^{1}H NMR (400 MHz in $CDCl_3$).

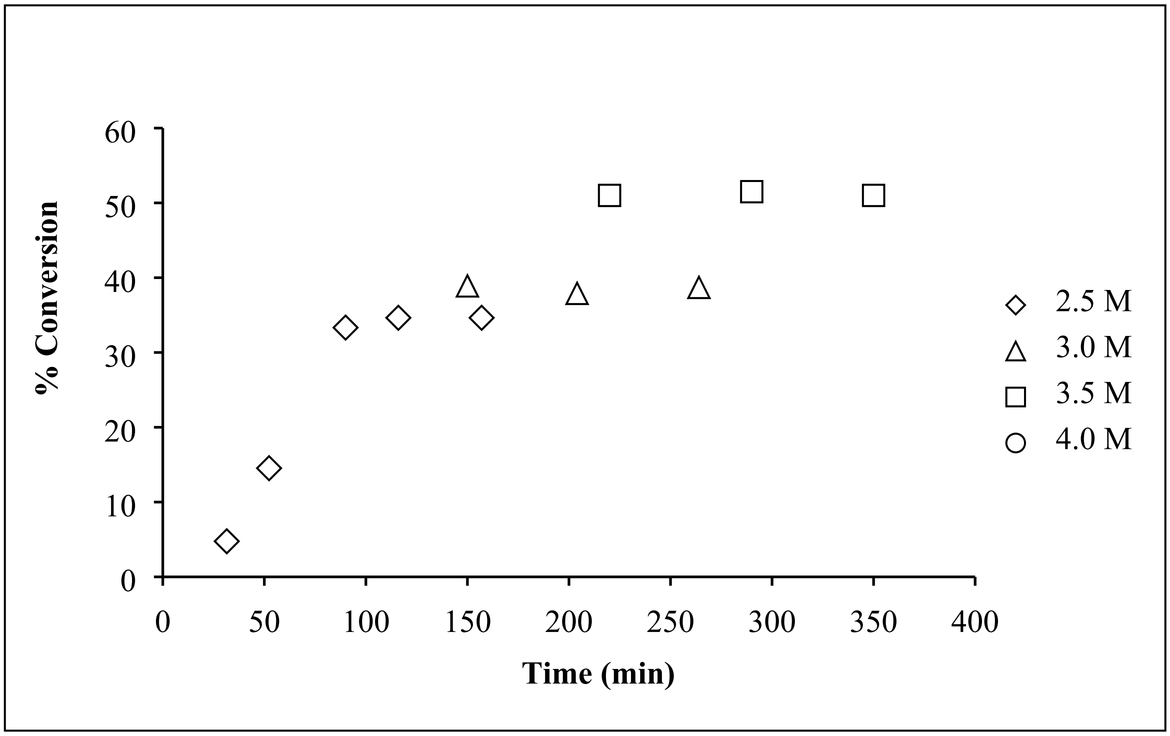

Figure S50. Equilibrium conversion of Poly(*rac*-3) with respect to time.

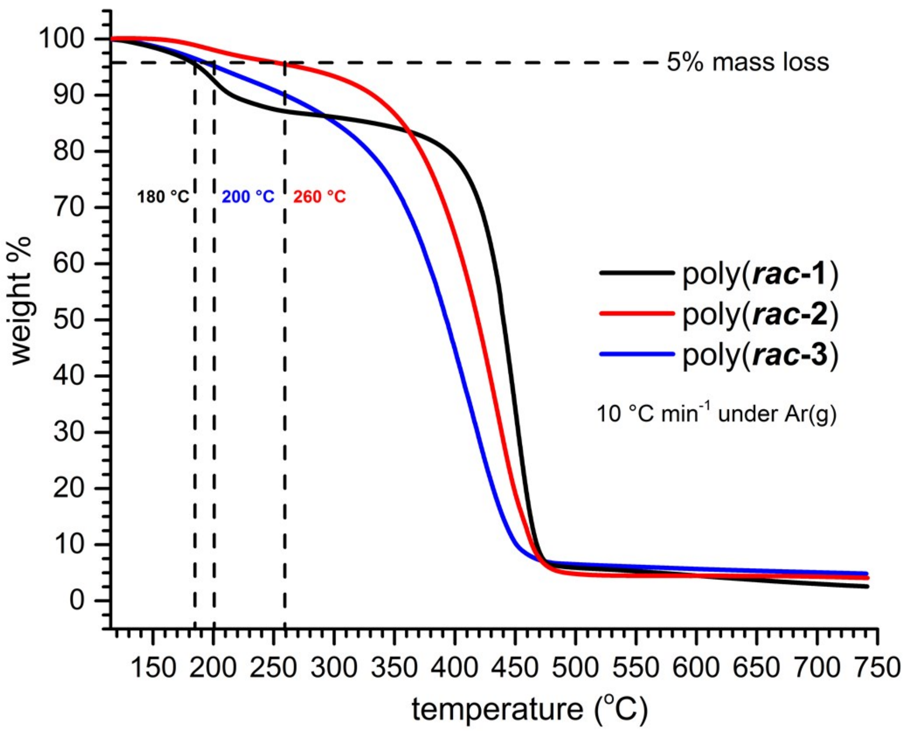

Figure S51. TGA analysis of poly(***rac*-1**), poly(***rac*-2**) and poly(***rac*-3**) after equilibration at 110 °C followed by heating at 10 °C min^{-1} to 750 °C under argon.

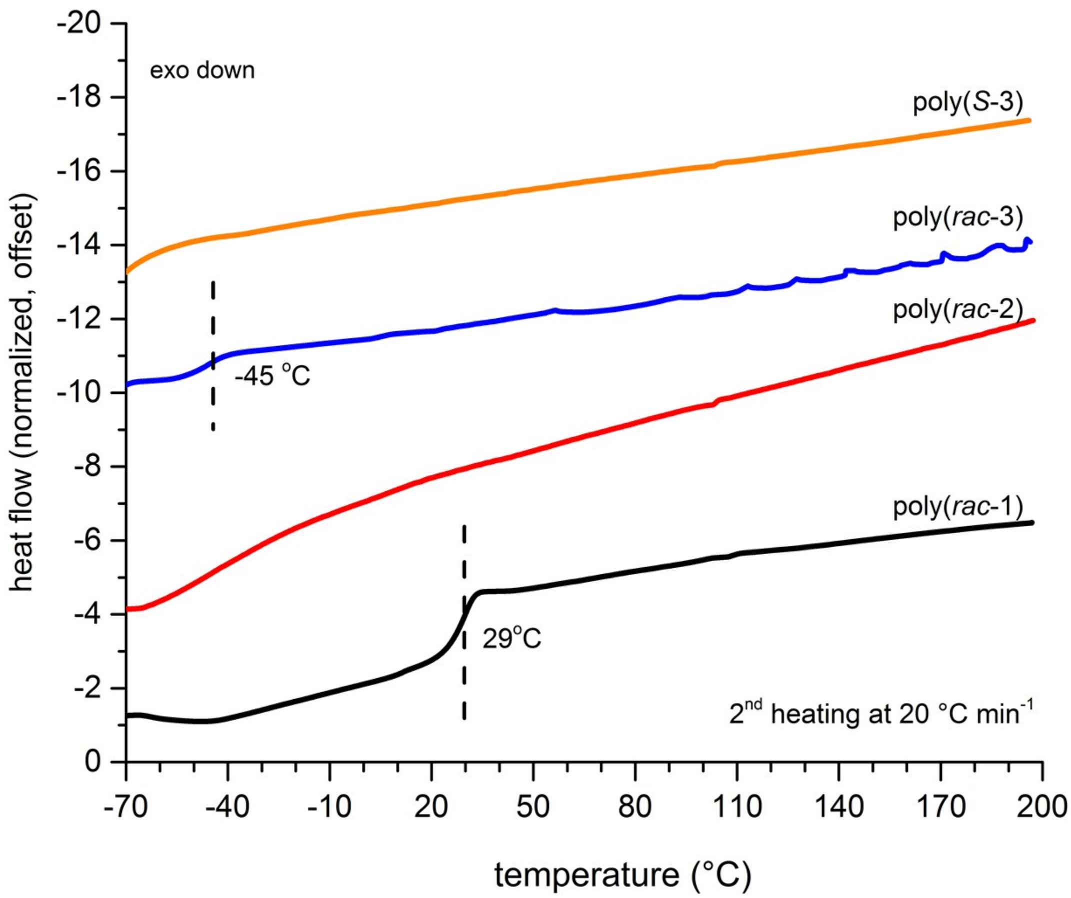

Figure S52. Differential scanning calorimetry thermograms of each polymer sample. The thermal range chosen was based on the minimum temperature for the instrument (-70 °C) and the temperature at which thermal decomposition of the polymer is suspected (~200 °C) based on TGA. Jagged baseline noise is present above 100 °C on some samples and was determined to be an artifact of the instrument by repeated cycles where this noise was found inconsistent.

References:

1. T. R. Hoye, C. S. Jeffrey and F. Shao, *Nature Protocols*, 2007, **2**, 2451.
2. B. M. Trost, D. L. Van Vranken and C. Bingel, *J. Am. Chem. Soc.*, 1992, **114**, 9327-9343.
3. S. Fuchs, V. Berl and J.-P. Lepoittevin, *European Journal of Organic Chemistry*, 2007, **2007**, 1145-1152.